



**HAL**  
open science

# Validation of Fast Neutron Reactors fertile blanket depletion calculations through the analysis of the DOUBLON experiment in PHENIX with TRIPOLI-4<sup>®</sup> and DARWIN3-SFR

Aurélie Calame, Jean-François Lebrat, Laurent Buiron

► **To cite this version:**

Aurélie Calame, Jean-François Lebrat, Laurent Buiron. Validation of Fast Neutron Reactors fertile blanket depletion calculations through the analysis of the DOUBLON experiment in PHENIX with TRIPOLI-4<sup>®</sup> and DARWIN3-SFR. *Annals of Nuclear Energy*, 2022, 169, pp.108947. 10.1016/j.anucene.2021.108947 . cea-03652125

**HAL Id: cea-03652125**

**<https://cea.hal.science/cea-03652125>**

Submitted on 3 May 2022

**HAL** is a multi-disciplinary open access archive for the deposit and dissemination of scientific research documents, whether they are published or not. The documents may come from teaching and research institutions in France or abroad, or from public or private research centers.

L'archive ouverte pluridisciplinaire **HAL**, est destinée au dépôt et à la diffusion de documents scientifiques de niveau recherche, publiés ou non, émanant des établissements d'enseignement et de recherche français ou étrangers, des laboratoires publics ou privés.

# Validation of Fast Neutron Reactors fertile blanket depletion calculations through the analysis of the DOUBLON experiment in Phenix with TRIPOLI-4® and DARWIN3-SFR

Aurélie CALAME, Jean-François LEBRAT\*, Laurent BUIRON

CEA, DES / IRESNE / DER / SPRC  
CEA de Cadarache, 13108 Saint Paul Lès Durance  
\*Email: [jean-francois.lebrat@cea.fr](mailto:jean-francois.lebrat@cea.fr)

## Abstract

A reliable assessment of the final inventory in the fertile blanket of a Fast Neutron Reactor is an important issue for fuel cycle physics, as it impacts safety, reprocessing and design studies. The performances of fertile blankets neutronics calculations is a long standing issue, as there are specificities in these regions that are quite challenging, especially for depletion codes.

The new CEA fuel depletion calculation package is DARWIN3-SFR, which incorporates the deterministic neutronics code APOLLO3® and the depletion module MENDEL. This paper details the validation of DARWIN3-SFR for fertile blanket calculations through the re-interpretation of the DOUBLON pin-irradiation in the Phenix reactor.

During this irradiation, nine pins are studied through isotopic ratios, which give us information about the depletion and, indirectly, the neutron flux calculations inside the blanket. This environment is especially challenging for neutronics codes, since there is a strong variation of the neutron energy and population over a short distance. Our recent analysis of TRAPU - which is a similar experiment, but in the core center - has proven DARWIN3-SFR to be reliable for the fuel depletion calculations of fissile subassemblies; nevertheless, its performances in the fertile blankets still require validation.

We observe that, once the calculated neutron flux level has been adjusted to the experiment through the  $^{148}\text{Nd}/^{238}\text{U}$  ratio, DARWIN3-SFR provides results similar to the reference stochastic code TRIPOLI-4®. However, both codes have difficulties to reproduce some of the measured isotopic ratios inside the fertile blanket. Whilst DARWIN3-SFR produces identical results for most of the isotopes analysed ( $^{234}\text{U}$ ,  $^{235}\text{U}$ ,  $^{236}\text{U}$ ,  $^{238}\text{Pu}$ ,  $^{239}\text{Pu}$ ,  $^{240}\text{Pu}$ ), variations of the neutron spectrum lead to some disparities for the production of  $^{241}\text{Pu}$  and  $^{242}\text{Pu}$ . Indeed, the low-energy flux estimation is higher with TRIPOLI-4® than with DARWIN3-SFR in the energy range where the  $^{240}\text{Pu}$  has a high capture cross section, which increases the calculated production of  $^{241}\text{Pu}$  and  $^{242}\text{Pu}$ .

DARWIN3-SFR and its predecessor DARWIN-2 are efficient at calculating the average neutron flux level over the entire fertile blanket. However, the results of the two codes show a strong pin-to-pin dispersion, resulting in a different shape of the neutron flux inside the blanket. With DARWIN3-SFR, the estimated neutron spectrum is softer than in DARWIN-2, which impacts the  $^{238}\text{U}$  capture and fission reaction rates and hence the production of plutonium.

## 1. Introduction

A reliable assessment of the final inventory in the fertile blanket of a Fast Neutron Reactor is an important issue for fuel cycle physics, as it impacts safety, reprocessing and design studies. The performances of fertile blankets neutronics calculations is a long standing issue (Beltranda, 1974; Corcuera, 1974; Soule, 1982), as there are specificities in these regions that are quite challenging, especially for depletion codes. Indeed, the blankets are irradiated in the peripheral regions, which are a transition region for the neutron flux. The magnitude of the latter is strongly attenuated, and the neutron energy spectrum softens with penetration. It was observed in several shielding experiments that the performances of calculation tools tend to deteriorate with penetration into the blanket (Grimm et al., 1998; Hill, 1997).

DARWIN3-SFR (Vaglio-Gaudard et al., 2016) is the CEA up-to-date deterministic tool for fuel depletion calculations. The CEA has developed it in order to replace DARWIN-2 for the calculations of decay heat, material balance, activity, etc.

DARWIN3-SFR incorporates APOLLO3® (Schneider et al., 2016) for the neutron flux calculation and the depletion module MENDEL (Lahaye et al., 2014). APOLLO3® already shows improved accuracy for neutron flux estimation and better computation performances than its predecessor ERANOS (Vidal et al., 2017). In addition, the propagation of the nuclear data uncertainties on the final inventory is now performed simply with the perturbations tools implemented in MENDEL.

DARWIN-2 - the predecessor of DARWIN3-SFR - had been validated over the years for Light Water Reactors (LWRs) (Eschbach et al., 2008; San Felice et al., 2013) as well as Fast Neutron Reactors (FNRs) calculations (Lebrat et al., 2015; Lebrat et al., 2018). The validation of DARWIN3-SFR has started recently for the fuel depletion calculations of core subassemblies (Calame et al., 2021), but the fertile blankets subassemblies have to be studied as well, since they will also have to be reprocessed in the future.

For this purpose, we present here the analysis of the DOUBLON PIE<sup>1</sup> of fertile subassemblies, which was performed in the Phenix reactor between 1979 and 1981. This experiment was aimed at validating the radial fertile blankets calculations and assessing the external regeneration gain. For this purpose, a study of two fertile subassemblies of the first and second rows of the radial fertile blanket was performed. Performing neutronic – and especially depletion – calculations in a reactor blanket is more challenging than inside the core, as the “fundamental mode” is not established and there is a strong variation of the neutron flux intensity and energy spectrum over a short distance.

We will compare the results we have obtained with DARWIN3-SFR to the experimental values, to the previous DARWIN-2 results and to the calculations performed with the stochastic code TRIPOLI-4® (Brun et al., 2004); the associated uncertainties will be detailed in each case.

## 2. Description of the DOUBLON irradiation experiment

Phenix is a sodium-cooled fast neutron reactor which was under exploitation between 1974 and 2009 and whose nominal thermal power of 563 MW was decreased to 350 MW in 1993.

DOUBLON is an irradiation experiment located in the radial fertile blanket and carried out from 1979 to 1981. Its initial purpose was the qualification of radial fertile blankets calculations - in particular

---

<sup>1</sup> Post-Irradiation Experiment

for the external regeneration gain determination - but it is also used for the validation of depletion calculations.

Figure 1 shows the two subassemblies involved in the DOUBLON experiment: FEF79 and FEG58.

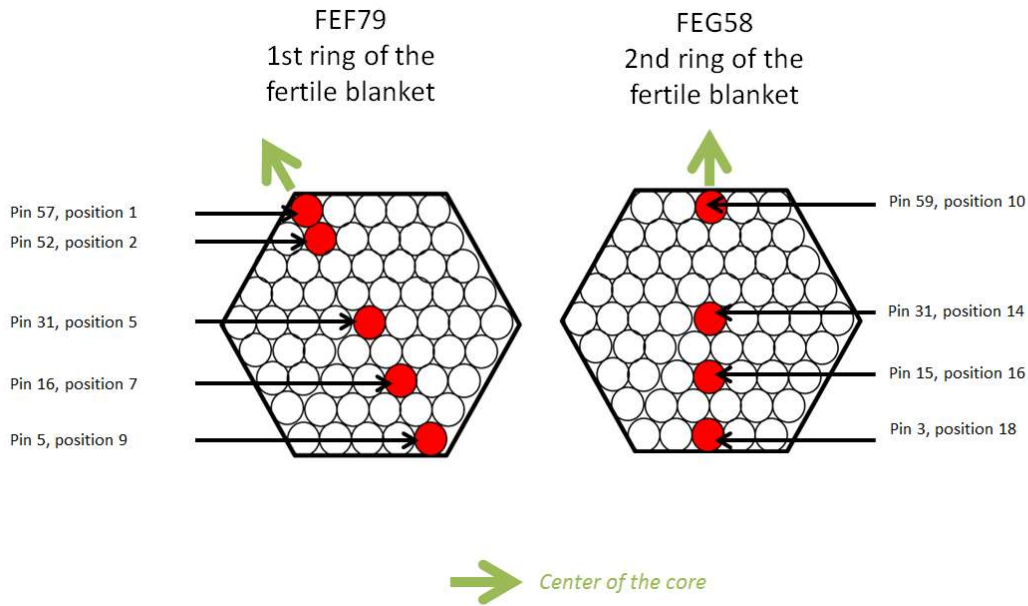


Figure 1: FEF79 and FEG58 subassemblies with the experimental pins in red

- The FEF79 subassembly is located in the first ring of the radial fertile blanket and was irradiated in position 27-17 from cycle 17 to 24, for 639.6 EFPD<sup>2</sup> (Figure 2). Five “regular” <sup>238</sup>U pins have been studied: number 57, 52, 31, 16, and 5. In order to simplify, we have re-numbered them 1, 2, 5, 7 and 9, by increasing distance from the core (Figure 1). Their <sup>235</sup>U content is 0.44% (atom percent).
- The FEG58 subassembly is located in the second ring of the radial fertile blanket and was irradiated in position 27-13 from cycle 13 to 22, for 758.5 EFPD (Figure 3). Four “regular” <sup>238</sup>U pins have been studied: number 59, 31, 15, and 3. In order to simplify, we have re-numbered them 10, 14, 16 and 18 (Figure 1). Their <sup>235</sup>U content is 0.47% (atom percent).

<sup>2</sup> Effective Full Power Day

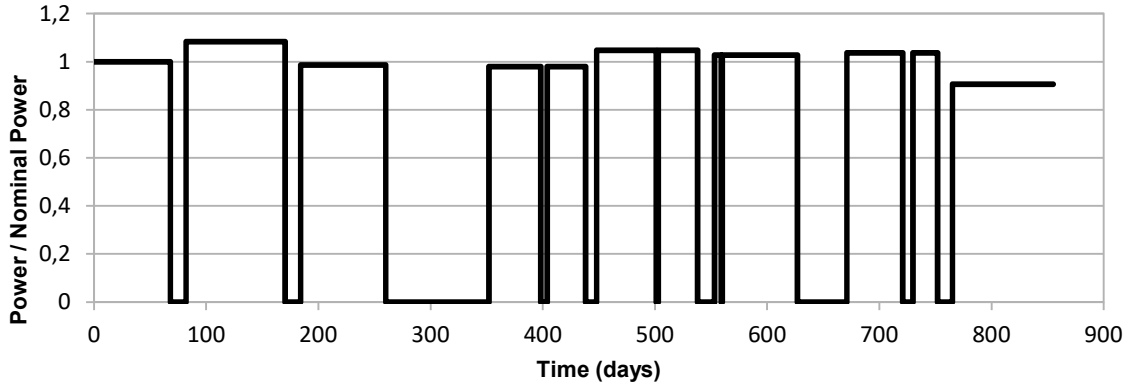


Figure 2: FEF79 subassembly irradiation history

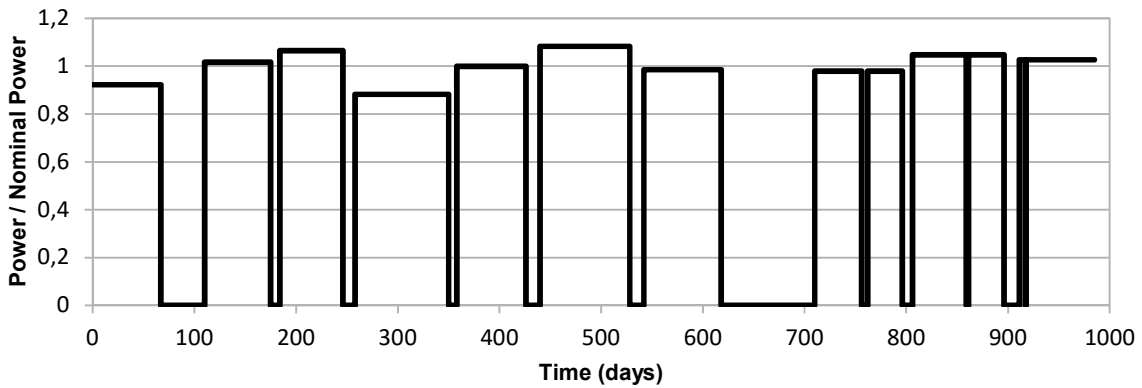


Figure 3: FEG58 subassembly irradiation history

For each experimental pin, several samples have been studied. For this purpose, each pin has been cut into samples that have been dissolved by a chemical process, and finally analyzed by mass spectroscopy in order to obtain isotopic ratios.

The following isotopic ratios have been measured:  $^{234}\text{U}/^{238}\text{U}$ ,  $^{235}\text{U}/^{238}\text{U}$ ,  $^{236}\text{U}/^{238}\text{U}$ ,  $^{239}\text{Pu}/^{238}\text{U}$ ,  $^{238}\text{Pu}/^{239}\text{Pu}$ ,  $^{240}\text{Pu}/^{239}\text{Pu}$ ,  $^{241}\text{Pu}/^{239}\text{Pu}$ ,  $^{242}\text{Pu}/^{239}\text{Pu}$  and finally  $^{148}\text{Nd}/^{238}\text{U}$ . The latter is used as a neutron flux indicator, allowing to adjust the calculated neutron flux if necessary<sup>3</sup>.

The experiment shows that the  $^{148}\text{Nd}/^{238}\text{U}$  ratio decreases by a factor 3 between the first and the last pin of the first ring subassembly (FEF79), and by a factor 2.3 for the second ring (FEG58). It means that, if both assemblies are adjusted to the same EFPD, the neodymium content varies from 260 to 40 ppm inside the blanket (Lebrat et al., 2015). It is obvious that reproducing such a strong flux variation over a short distance is a real challenge for calculation codes.

<sup>3</sup> The  $^{148}\text{Nd}$  inside the pins is produced by fission reactions, whose rate is proportional to the local neutron flux

### 3. The modelling of the irradiation

The modeling of the DOUBLON irradiation with DARWIN3-SFR and TRIPOLI-4® is similar to the one we have performed in our previous work on the TRAPU irradiation, in the core center of Phenix (Calame et al., 2021).

#### 3.1 The modeling of the irradiation with DARWIN3-SFR

DARWIN3-SFR (Vaglio-Gaudard et al., 2016) is the CEA up-to-date deterministic tool for fuel depletion calculations. The CEA has developed it in order to replace DARWIN-2 for the calculations of decay heat, material balance, activity, etc.

Figure 4 shows the DARWIN3-SFR calculation sequence, which incorporates APOLLO3® (Schneider et al., 2016) for the neutron flux calculation and the depletion module MENDEL (Lahaye et al., 2014). APOLLO3® already shows improved accuracy for neutron flux estimation and better computation performances than its predecessor ERANOS (Vidal et al., 2017). In addition, the propagation of the nuclear data uncertainties on the final inventory is now performed simply with the perturbations tools implemented in MENDEL.

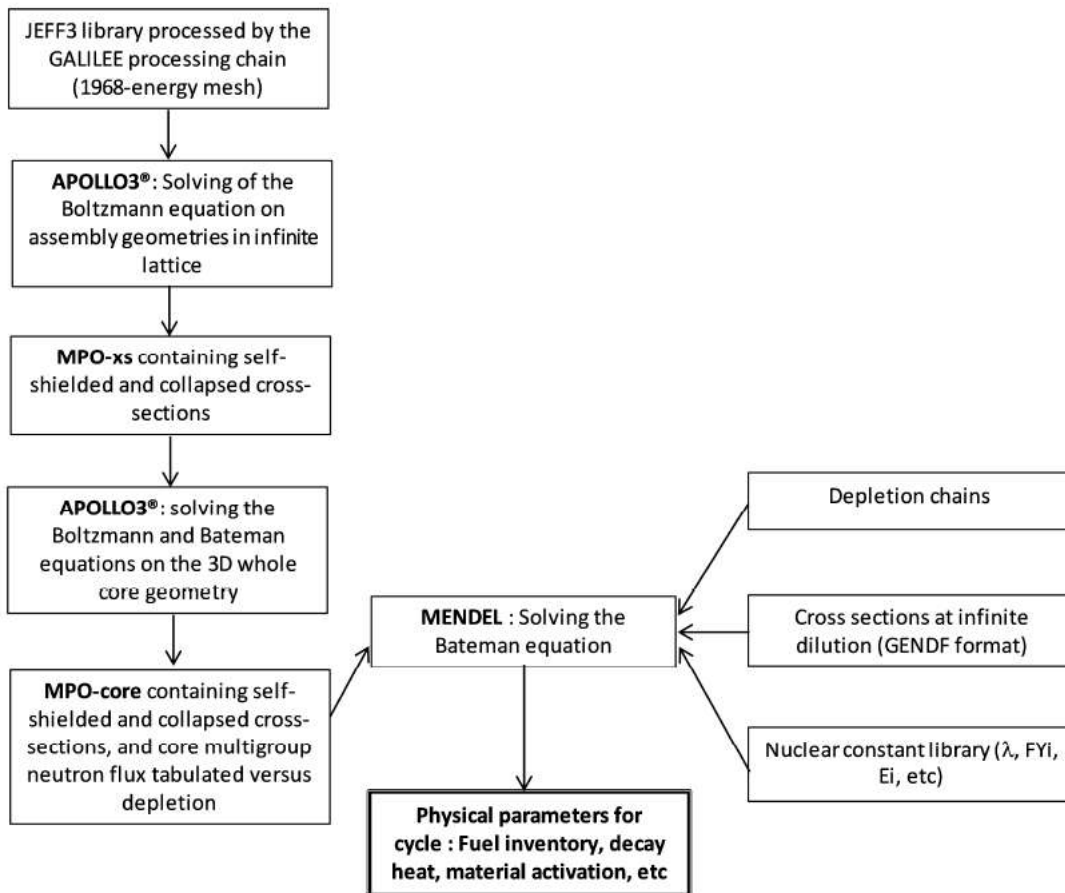


Figure 4: Description of the code chaining relative to the APOLLO3® + MENDEL route of DARWIN3-SFR (Vaglio-Gaudard et al., 2016)

Details about the APOLLO3® neutron flux calculation we have performed are provided in (Calame et al., 2021). In short:

- The lattice calculation produces the effective homogenized cross sections at the subassembly level,
- These cross sections are used during the core calculation by the TDT<sup>4</sup> solver with a 1760 groups energy mesh, followed by a condensation to 33 groups.

At core scale, APOLLO3® offers several numerical solvers to solve the Boltzmann equation: MINOS (Baudron et al., 2007), PASTIS (Lewis et al., 1986) and MINARET (Moller et al., 2011). Among them - which are equally efficient to master flux calculation for depletion purpose - MINOS and PASTIS are not able to manage unstructured geometries. In the present case, only MINARET - using discrete ordinates computational methods with adaptive triangular mesh - has the capability to treat unstructured geometries, in which the fuel pellets granularity is preserved at core scale.

This particular feature is of prime interest for the present study, in which experimental values are available for dedicated pellets across the fertile sub-assemblies. Treating the sub-assembly in a homogenous way - such as needed for MINOS or PASTIS - would introduce additional approximations and thus a potential numerical bias. In MINARET, we have set the angular order equal to 4 and the radial / axial orders equal to 1, which corresponds to a linear expansion of the flux. This low order is counter-balanced by a refined triangular mesh (centimeter scale) around the fertile pellet for the dedicated sub-assemblies to take into account the flux gradient in those core areas.

The core calculation are performed in a semi-heterogeneous geometrical modelling: each subassembly is homogenized radially, while keeping its axial heterogeneity. The experimental pins have been modeled separately - thanks to the APOLLO3® unstructured geometries - as shown on Figure 5 and Figure 6.

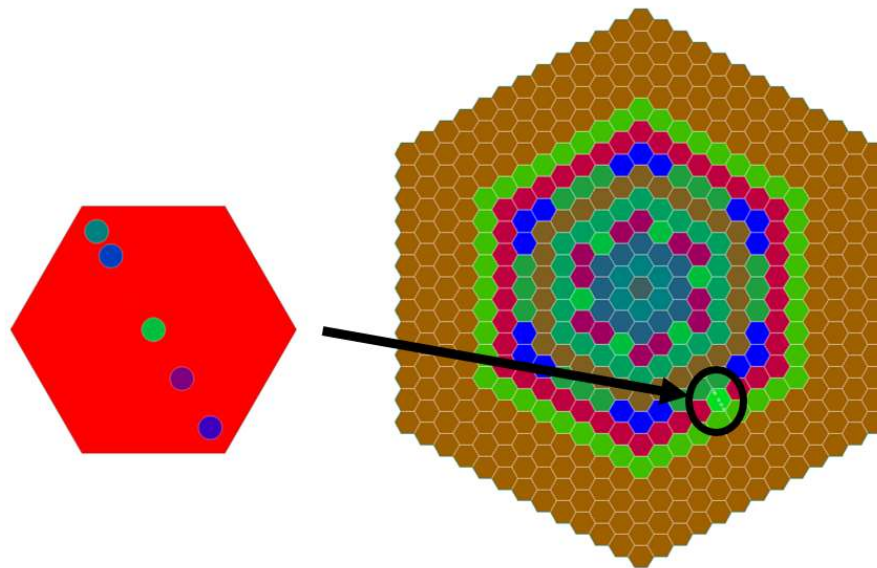


Figure 5: *Geometrical description of the FEF79 subassembly inside the PHENIX reactor with APOLLO3®*

---

<sup>4</sup> Two / Three Dimensional Transport

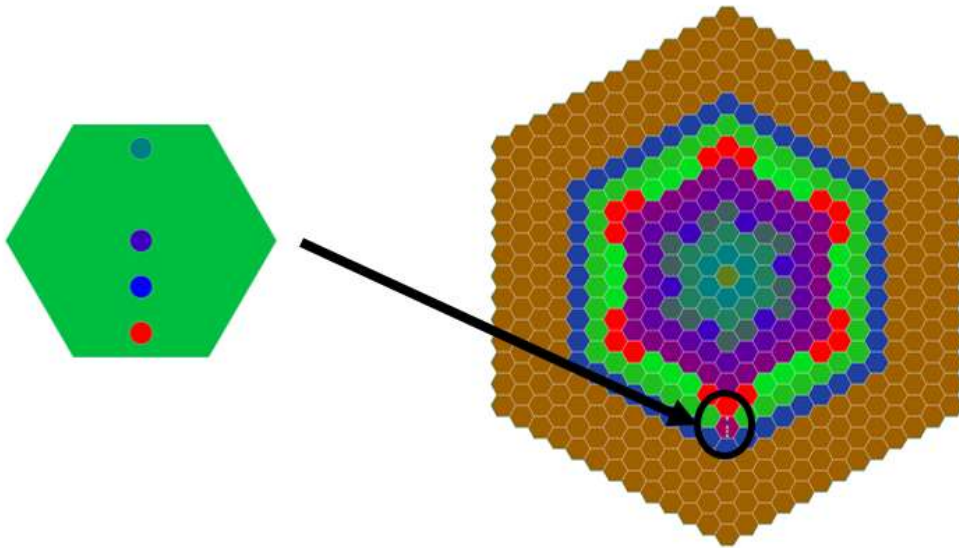


Figure 6: *Geometrical description of the FEG58 subassembly inside the PHENIX reactor with APOLLO3®*

### 3.2 The modeling of the irradiation with TRIPOLI-4®

In addition to DARWIN3-SFR, we have also simulated the DOUBLON experiment with the “reference” stochastic code TRIPOLI-4®, according to the geometrical modeling of Figure 7.

Whereas a deterministic code has calculation biases because of the associated models approximations, a stochastic code such as TRIPOLI-4® performs only minimal approximation for the neutron flux calculation: the associated calculation result can be considered as a “reference”, as the only discrepancies with measurements can be attributed to biases in the nuclear data. Like in DARWIN3-SFR, the depletion calculations in TRIPOLI-4® are performed by the MENDEL module.

In order to find a good compromise between calculation time and accuracy of the results, our simulations consisted in 5000 batches of 5000 neutrons for each time step.

In our spatial modeling of the irradiation, the subassemblies are homogenized radially – but their axial structure is fully described (7A). The subassemblies of interest are fully described in their fertile area (Figure 7B), but only the samples inside the pins of interest are depleted – which corresponds to five samples for the FEF79 simulation and four samples for the FEG58 simulation.

The nuclear data library we have used is JEFF-3.1.1 (Santamarina et al., 2009) with a temperature of 20°C, as it constitutes the reference data used in FNR neutronics calculations at CEA and has proven good performances when associated with ERANOS (Lebrat et al., 2011).



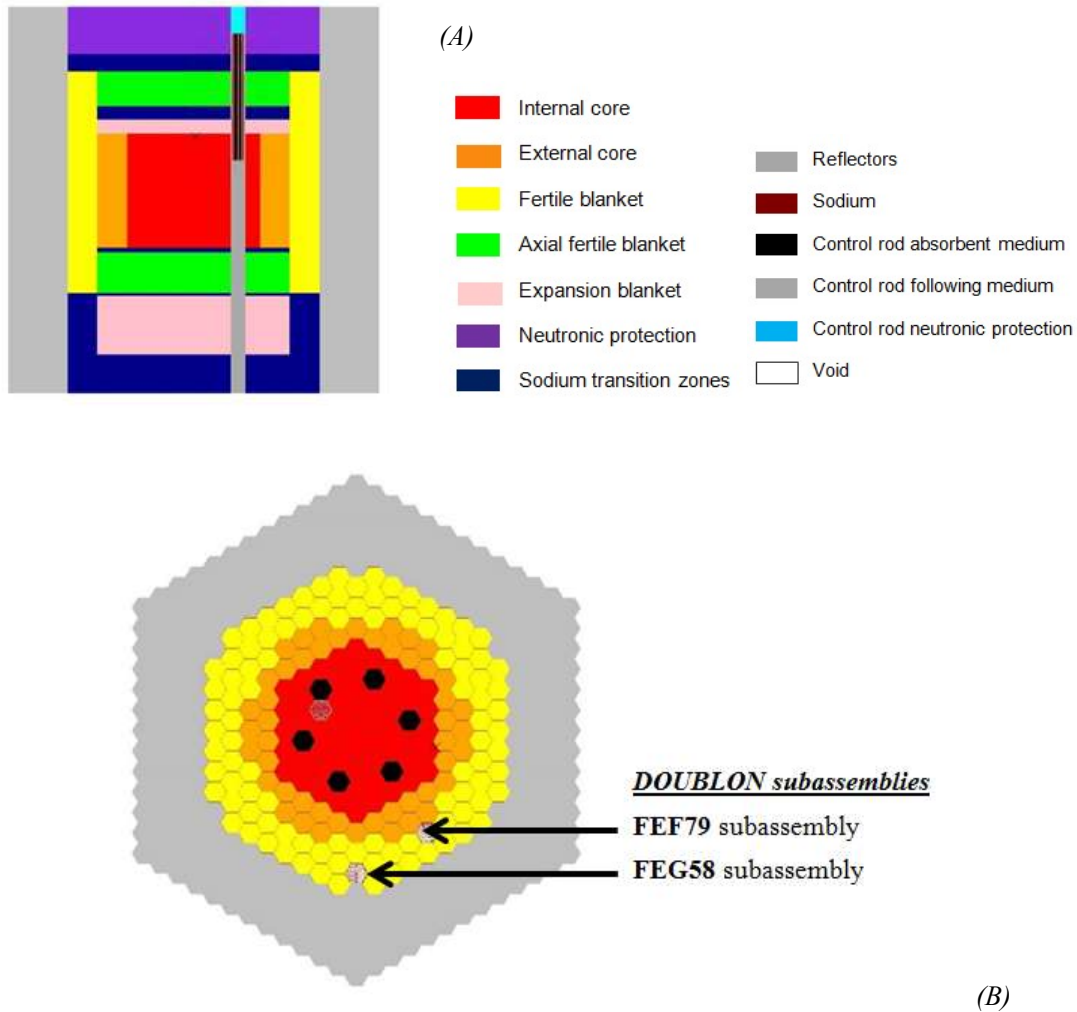


Figure 7: TRIPOLI-4® semi-heterogeneous modelling of the DOUBLON irradiation

### 3.3 The description of the irradiation history

The irradiation histories of both the FEF79 and FEG58 subassemblies have been accurately modeled (see Figure 2 and Figure 3). Since both subassemblies have not been irradiated during the same reactor cycles, we had to perform the corresponding depletion calculations separately (see Figure 8). However, the results will be presented on the same graph.

« FEF » modelling : modelling of the FEF79 subassembly, with its irradiation history from cycle 17 to 24.

« FEG » modelling : modelling of the FEG58 subassembly, with its irradiation history from cycle 13 to 22

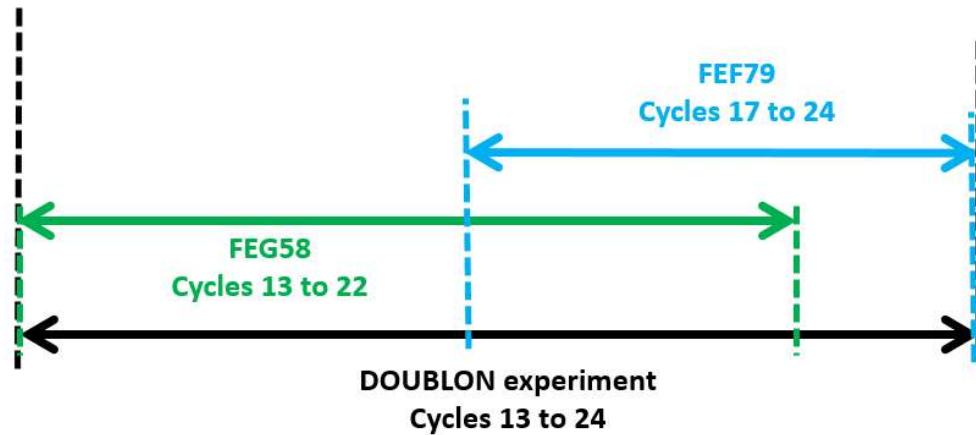


Figure 8: Irradiation history of the FEF79 and FEG58 subassemblies during the DOUBLON experiment

Indeed, even though these subassemblies are not aligned with respect to the core center and are not adjacent to each other, they are at increasing distances from the center of the core. The experimental pins are therefore virtually aligned with each other in the axis of the core center (see Figure 9 and Figure 10).

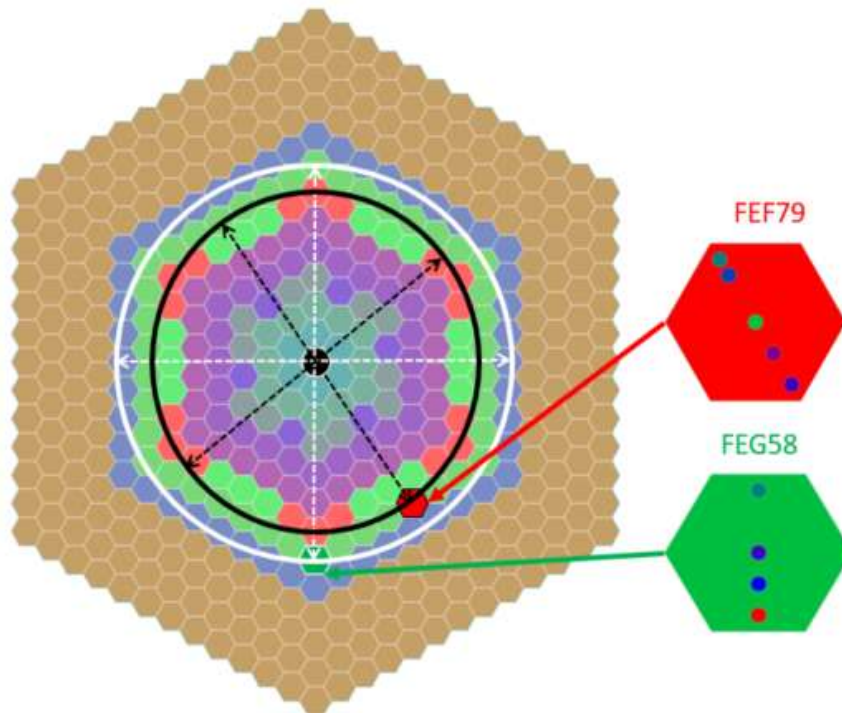


Figure 9: Position of the FEF79 and FEG58 subassemblies inside the core and alignment of the experimental pins

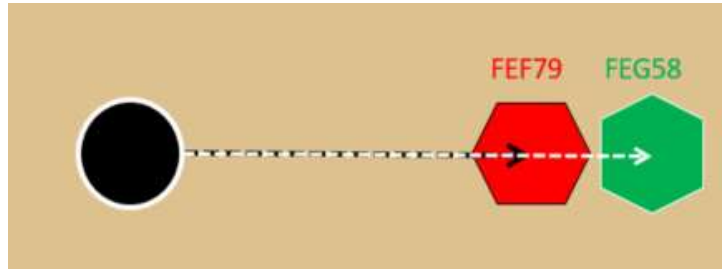


Figure 10: Virtual subassemblies alignment

Thus, by symmetry and thanks to the increasing distances between the pins and the core center (Figure 11), it can be considered that the FEF79 and FEG58 subassemblies and their respective experimental pins are virtually aligned. In addition, thanks to the flux adjustment, the calculated values in the two assemblies can be compared to each other, despite their different irradiation time.

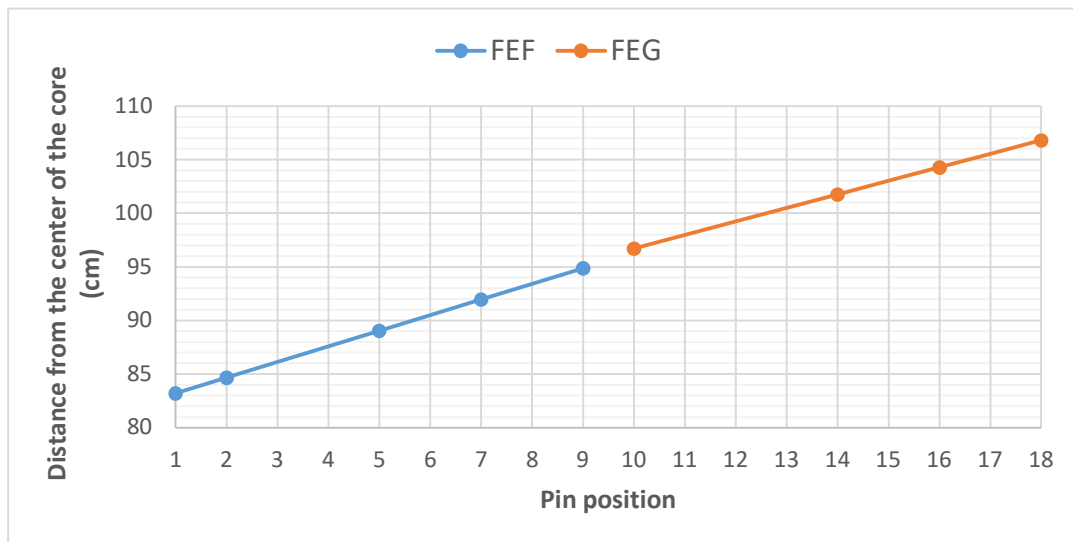


Figure 11: Distance between each experimental pin and the core center

### 3.4 Influence of the modification of the subassemblies environment

During the irradiation, the environment of the FEF79 and FEG58 subassemblies was unfortunately modified:

- In position 25-14, the fertile subassembly was replaced by a fissile subassembly in the 20<sup>th</sup> and 21<sup>st</sup> cycles (from 06/23/1980 to 01/04/1980).
- In position 26-15, the fertile subassembly was replaced by a fissile subassembly from the 19<sup>th</sup> to the 22<sup>nd</sup> cycles (from 11/01/1980 to 05/04/1981).

These modifications can affect the neutron flux in the subassemblies of the DOUBLON experiment, and in particular the FEG58 subassembly, as can be seen in Figure 12.

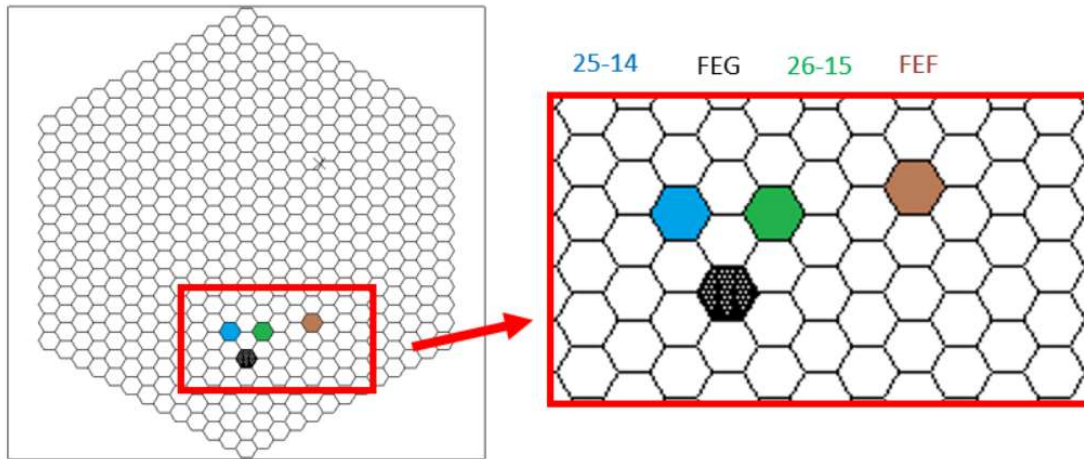


Figure 12: Positions 25-14 and 26-15, where some subassemblies were replaced by others during the experiment

The FEG58 subassembly was obviously more directly impacted by these modifications<sup>5</sup> and two different modelings were tested with TRIPOLI-4® for the FEG58 subassembly calculation<sup>6</sup>:

- 1) Without taking into account these changes in the environment (“constant loading plan”).
- 2) With taking them into account for the FEG58 subassembly (“evolving loading plan”).

The  $^{148}\text{Nd}/^{238}\text{U}$  isotopic ratio calculated with both modelings is shown on Figures 13. We observe that one curve can be deduced from the other increased by the same multiplying factor for all the pins. Since a flux adjustment will be performed in any case in order to match the calculated  $^{148}\text{Nd}/^{238}\text{U}$  ratio to the measured one, we can keep the approximation of the “constant” loading plan in our calculations.

<sup>5</sup> we consider that the FEF79 subassembly was not impacted

<sup>6</sup> except for these two positions, the rest of the loading plan is considered constant

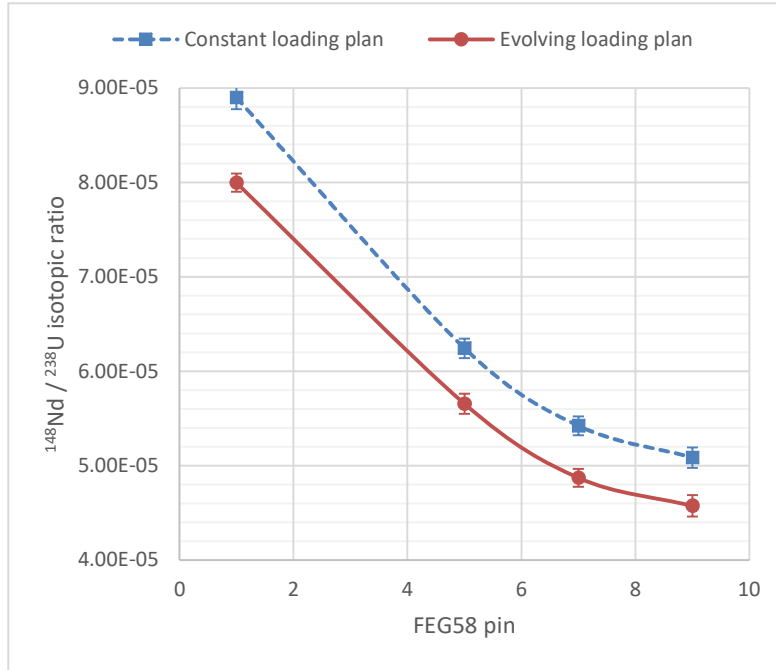


Figure 13:  $^{148}\text{Nd}/^{238}\text{U}$  isotopic ratio for the pins of the FEG58 subassembly with a *constant* or *evolving* loading plan

#### 4. Comparative analysis of the experiment with DARWIN3-SFR, DARWIN-2 and TRIPOLI-4®

The DOUBLON experiment was previously analyzed (Lebrat et al., 2015) with the DARWIN-2 package (Tsilanzara et al., 2000), based on the ERANOS neutronic code (Ruggieri et al., 2006). We will compare these results with those we now obtain with DARWIN3-SFR and TRIPOLI-4® and we will also study the effect of using the JEFF-3.2 nuclear data library (NEA, 2016) instead of JEFF-3.1.1.

##### 4.1 Adjustment of the calculated irradiation neutron flux to the experiment

The  $^{148}\text{Nd}$  is a stable fission product produced in our case by some fissions of  $^{235}\text{U}$ ,  $^{238}\text{U}$  and  $^{239}\text{Pu}$ . At the end of the irradiation, the amount of this nuclide is proportional to the integrated neutron flux, or in other words to the burnup. During the interpretation of PIEs, an adjustment of the calculated neutron flux is usually performed in order to match the calculated  $^{148}\text{Nd}/^{238}\text{U}$  ratio to the experimental value: this way, a potential bias on the calculated flux level will not propagate to the fuel depletion calculations.

##### 4.2 Production pathway of the isotopes of interest

The INVERSION module of DARWIN-2 provides the production pathway of the heavy nuclides measured at the end of the irradiation. The major contributions are shown in Table 1.

Table 1: Production pathways of the different nuclides measured after irradiation

Heavy Nuclide	Proportion (%)	Provenance
$^{238}\text{Pu}$	~58.6	$^{238}\text{U}(n, 2n) \rightarrow ^{237}\text{U}(\beta^-) \rightarrow ^{237}\text{Np}(n, \gamma) \rightarrow ^{238}\text{Np}(\beta^-) \rightarrow ^{238}\text{Pu}$
	~32.4	$^{236}\text{U}(n, \gamma) \rightarrow ^{237}\text{U}(\beta^-) \rightarrow ^{237}\text{Np}(n, \gamma) \rightarrow ^{238}\text{Np}(\beta^-) \rightarrow ^{238}\text{Pu}$
$^{239}\text{Pu}$	~100	$^{238}\text{U}(n, \gamma) \rightarrow ^{239}\text{U}(\beta^-) \rightarrow ^{239}\text{Np}(\beta^-) \rightarrow ^{239}\text{Pu}$
$^{240}\text{Pu}$	~96.7	$^{238}\text{U}(n, \gamma) \rightarrow ^{239}\text{U}(\beta^-) \rightarrow ^{239}\text{Np}(\beta^-) \rightarrow ^{239}\text{Pu}(n, \gamma) \rightarrow ^{240}\text{Pu}$
$^{241}\text{Pu}$	~95.7	$^{238}\text{U}(n, \gamma) \rightarrow ^{239}\text{U}(\beta^-) \rightarrow ^{239}\text{Np}(\beta^-) \rightarrow ^{239}\text{Pu}(n, \gamma) \rightarrow ^{240}\text{Pu}(n, \gamma) \rightarrow ^{241}\text{Pu}$
$^{242}\text{Pu}$	~93.4	$^{238}\text{U}(n, \gamma) \rightarrow ^{239}\text{U}(\beta^-) \rightarrow ^{239}\text{Np}(\beta^-) \rightarrow ^{239}\text{Pu}(n, \gamma) \rightarrow ^{240}\text{Pu}(n, \gamma) \rightarrow ^{241}\text{Pu}(n, \gamma) \rightarrow ^{242}\text{Pu}$

It appears that the heavy nuclides are produced exclusively during the TRAPU irradiation by successive reactions on  $^{238}\text{U}$  and consequently their final amounts will very likely be sensitive to modeling / calculation biases.

### 4.3 Calculation of the isotopic ratios and the associated uncertainties

After the flux adjustment based on the  $^{148}\text{Nd}/^{238}\text{U}$  ratio, we compare the various isotopic ratios that we have calculated with TRIPOLI-4®, DARWIN-2 and DARWIN3-SFR to the measured values by the means of C/E<sup>7</sup> ratios. The 1 $\sigma$  uncertainties on these ratios account for the experimental uncertainty of typically 0.5% and the statistical dispersion of the stochastic calculations results.

For each isotopic ratio, the IncerD module of MENDEL (Lahaye et al., 2018) performs the propagation of the uncertainties on the nuclear data involved in the calculation<sup>8</sup> to the final inventory of each nuclide.

IncerD uses the covariance data from the COMAC-v2 database (Archier et al., 2014), which includes all the nuclear data and covariance matrices associated to the microscopic cross sections, decay data, fission yields<sup>9</sup>, fission neutron spectra and multiplicities in the adequate 33 groups energy mesh. These data cover most of the major actinides, fission products and structure materials involved in our calculations. The relative uncertainty on an isotopic ratio is calculated as the sum of the relative uncertainties on the two concentrations, which are estimated by IncerD.

### 4.4 Comparative analysis of the DARWIN3-SFR and TRIPOLI-4® results

A comparison of the experimental values to the calculations results of DARWIN3-SFR and TRIPOLI-4® is performed. In both calculations, only the concentrations of DOUBLON pins are depleted, the core temperature is 20 °C and the JEFF-3.1.1 (Santamarina et al., 2009) nuclear data library is used.

#### 4.4.1 Analysis of the $^{148}\text{Nd}$ production

Figure 14 shows the C/E of the  $^{148}\text{Nd}/^{238}\text{U}$  ratio for the different experimental pins. The 1 $\sigma$  nuclear data uncertainty associated with the DARWIN3-SFR calculation is around 7% and dominated by the fast spectrum independent fission yields of  $^{238}\text{U}$  to  $^{148}\text{Ce}$  and  $^{148}\text{La}$ , which both decay into  $^{148}\text{Nd}$  by successive  $\beta$  decays.

<sup>7</sup> Calculation over Experiment

<sup>8</sup> This concerns the decay constants, branching ratios, cross sections, independent fission yields

<sup>9</sup> At this point, COMAC does not include the covariances between the independent fission yields

The TRIPOLI-4® and DARWIN3-SFR results are compatible within these uncertainties, except for the last pin where a drop is observed with DARWIN3-SFR. It appears that DARWIN3-SFR calculates the evolution of the neutron flux throughout the blanket in a way similar to TRIPOLI-4®.

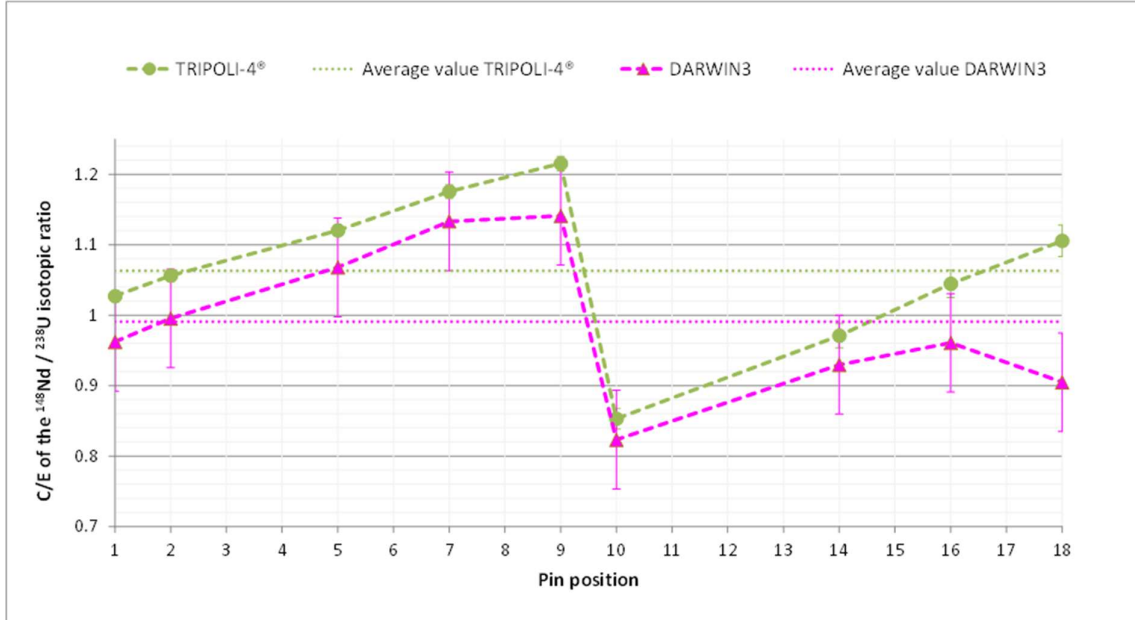


Figure 14: C/E of the  $^{148}\text{Nd}/^{238}\text{U}$  isotopic ratio obtained with TRIPOLI-4® and DARWIN3-SFR ( $1\sigma$  uncertainties)

Nevertheless, large pin-to-pin variations are observed, especially at the interface between the two subassemblies. In this zone, the C/E varies from 1.2 to 0.8 over a very short distance, which shows the limitations of our depletion codes to reproduce the measured neutron flux evolution within the fertile radial blanket. Indeed, with a perfect<sup>10</sup> calculation code and perfect nuclear data, the curve should be flat.

However, the average C/E estimated with DARWIN3-SFR is very close to one, which shows that the average neutron flux in the blanket is well estimated, despite the important spatial variations.

#### 4.4.2 Production of other nuclides

For the analysis of the production of other nuclides, only one pin will be analyzed. Indeed, performing a neutron flux adjustment (which is an iterative procedure) with TRIPOLI-4® would be too much time consuming and is not reasonably achievable in the frame of this work. We chose the pin in the 14<sup>th</sup> position (i.e. the 2<sup>nd</sup> pin of the FEG58 subassembly), since for this pin the C/E of the  $^{148}\text{Nd}/^{238}\text{U}$  isotopic ratio with TRIPOLI-4® is the closest to one (see Figure 15).

A flux adjustment performed with DARWIN3-SFR makes it possible to obtain the same C/E of the  $^{148}\text{Nd}/^{238}\text{U}$  isotopic ratio for this pin, as can be seen in Table 2. We did not know upstream which flux adjustment factor was optimal for this type of analysis. So after having carried out several tests, we focused on the factor which makes it possible to obtain the DARWIN3-SFR C/E of

<sup>10</sup> i.e. without any calculation bias

$^{148}\text{Nd}/^{238}\text{U}$  simultaneously closest to the TRIPOLI-4® value and to one. This factor (0.96) was obtained by adjusting the neutron flux with the mean value of the C/E of  $^{148}\text{Nd}/^{238}\text{U}$ .

Table 2: Determination of the neutron flux adjustment factor

« FEG-14 » 2 <sup>nd</sup> pin of FEG58, 14 <sup>th</sup> pin of DOUBLON	Flux adjustment factor	C/E of $^{148}\text{Nd}/^{238}\text{U}$
TRIPOLI-4®	–	0.97
DARWIN3-SFR (without any adjustment)	–	0.93
DARWIN3-SFR (adjusted with the mean value of the C/E)	$f = \frac{1}{\left(\frac{C}{E}\right)_{mean}}$	0.96
DARWIN3-SFR (adjusted with the C/E value of the 14 <sup>th</sup> pin)	$f = \frac{1}{\left(\frac{C}{E}\right)_{14^{th} \text{ pin}}}$	1.03

Figure 15 compares the results of DARWIN3-SFR with those of TRIPOLI-4® for the 14<sup>th</sup> pin of the FEG58 subassembly, after the flux adjustment with the mean value of the C/E. This pin has now a similar C/E of  $^{148}\text{Nd}/^{238}\text{U}$  between TRIPOLI-4® and DARWIN3-SFR and close to 1 in both cases. This means that the calculated neutron flux now matches the experimental one in this position and that we can analyze the other isotopic ratios.

We can observe on Figure 15 that:

- The C/E for  $^{234}\text{U}/^{238}\text{U}$ ,  $^{235}\text{U}/^{238}\text{U}$ ,  $^{236}\text{U}/^{238}\text{U}$ ,  $^{239}\text{Pu}/^{238}\text{U}$ ,  $^{238}\text{Pu}/^{239}\text{Pu}$ ,  $^{240}\text{Pu}/^{239}\text{Pu}$  and  $^{242}\text{Pu}/^{239}\text{Pu}$  and compatible between DARWIN3-SFR and TRIPOLI-4®, with respect to the associated  $1\sigma$  uncertainties.
- There is a discrepancy for the production of  $^{241}\text{Pu}$ , but the values would be compatible if  $2\sigma$  uncertainties were considered.



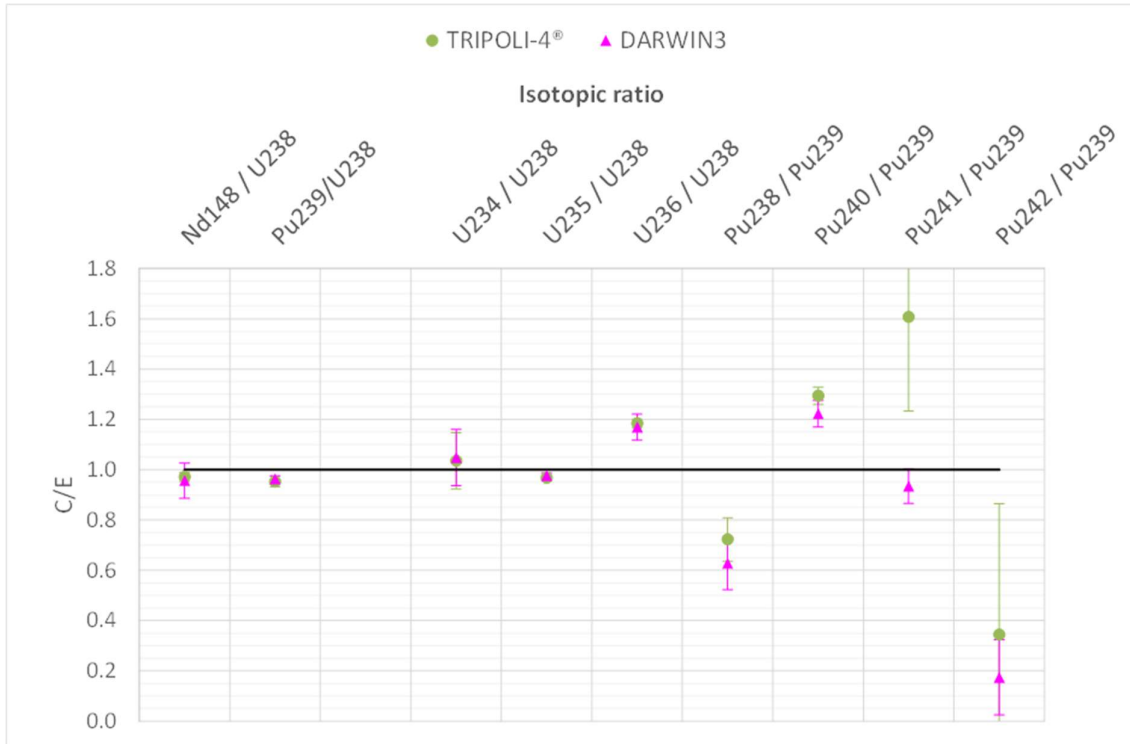


Figure 15: C/E of the isotopic ratios for the 14th pin ( $1\sigma$  uncertainties)

By studying the C/E of Figure 15 and the production pathways of the different nuclides in Table 1, the following analysis can be made:

- The  $^{238}\text{Pu}$  is an isotope whose production is sensitive to neutron spectrum. Indeed, Table 1 shows that this nuclide is produced mainly by the  $^{238}\text{U}(n, 2n)$  reaction, which has a high-energy threshold of 6 MeV. The analysis of the  $^{237}\text{Np}$  production in the TRAPU experiment (Calame et al., 2021) showed a potential underestimation of the  $^{238}\text{U}(n, 2n)$  cross section, which could explain the underestimation of the  $^{238}\text{Pu}$  production that we observe in the DOUBLON experiment with both TRIPOLI-4® and DARWIN3-SFR.
- The production of  $^{240}\text{Pu}$  is compatible between both calculation codes (within their uncertainties), but is overestimated compared to the experiment. Table 1 shows that this nuclide is produced by the  $^{239}\text{Pu}(n, \gamma)$  reaction. Figure 16 and 17 show that this reaction has a low energy resonance (below 1eV), where the neutron flux<sup>11</sup> is very low and probably poorly estimated by both our neutronic calculation codes, according to the huge discrepancy between the TRIPOLI-4® and APOLLO3® flux estimations.
- The same analysis stands for the production of  $^{241}\text{Pu}$  and  $^{242}\text{Pu}$ , who are produced by successive capture reactions on the  $^{240}\text{Pu}$ , as shown in Table 1: The calculation biases that we have described for the production of  $^{240}\text{Pu}$  are cumulated for these nuclides.

<sup>11</sup> Figure 19 and 20 show the neutron flux averaged over all the experimental pins

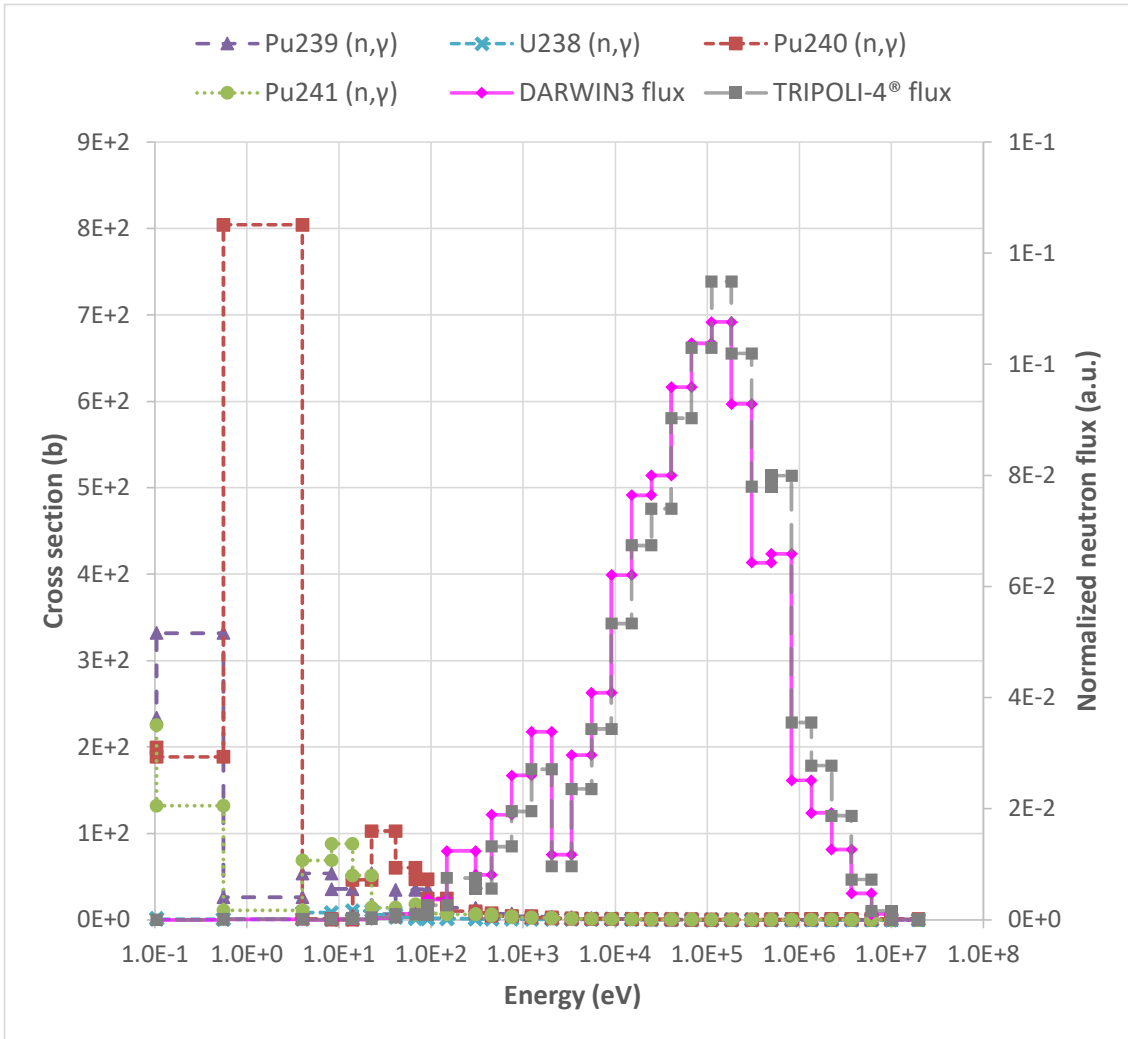


Figure 16: Comparison of the neutron flux and several reactions cross sections with DARWIN3-SFR and TRIPOLI-4® (linear scale)

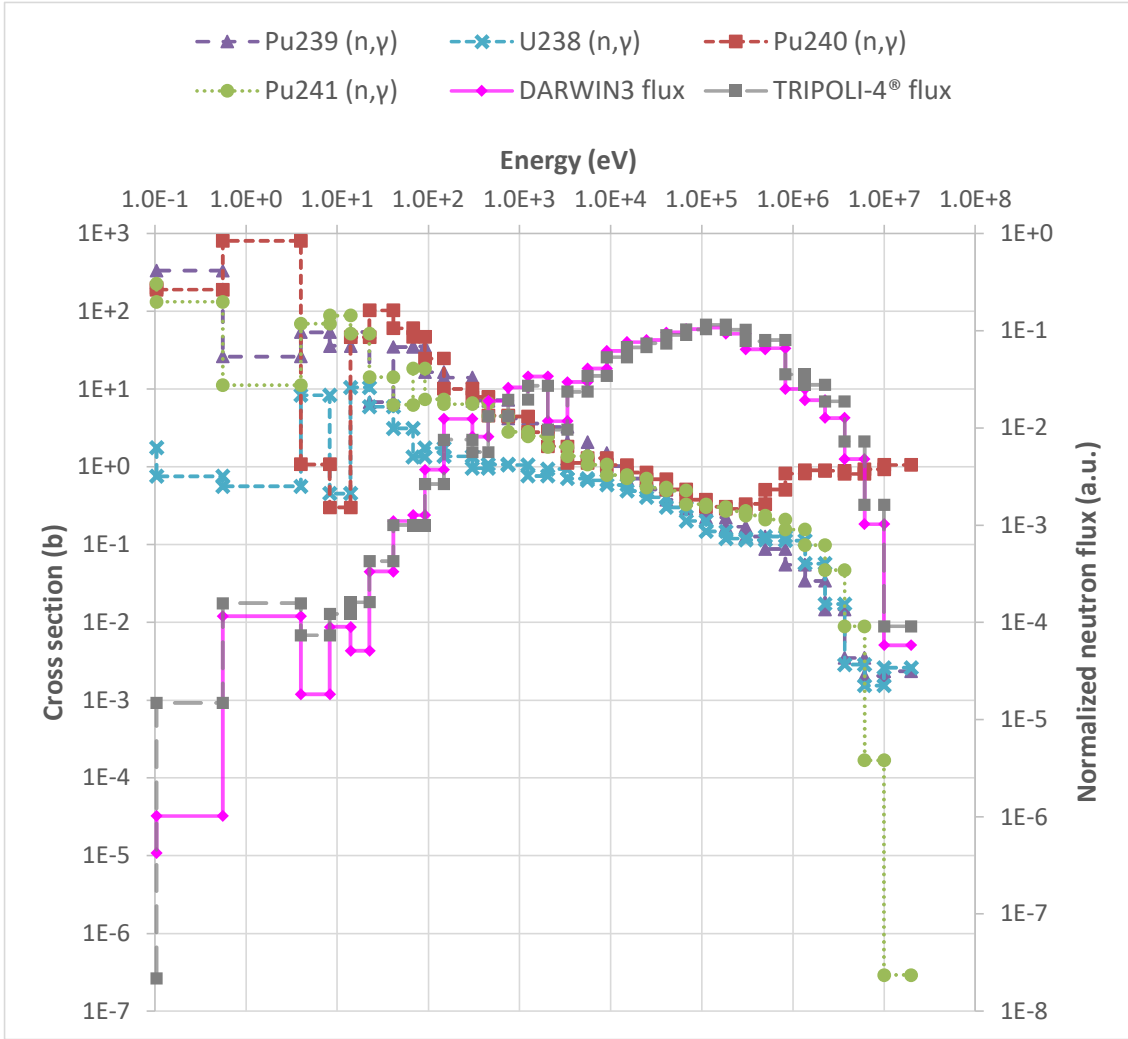


Figure 17: Comparison of the neutron flux and several reactions cross sections with DARWIN3-SFR and TRIPOLI-4® (logarithmic scale)

During the irradiation, the  $^{240}\text{Pu}$ ,  $^{241}\text{Pu}$  and  $^{242}\text{Pu}$  are produced in very small amounts (see Table 3), as they are not present in the initial composition of the fertile pins. The disparities observed between TRIPOLI-4® and DARWIN3-SFR for the production of these nuclides can be explained by differences in the calculated neutron energy spectrum. For instance, we notice on Figures 16 and 17 that the estimated low-energy neutron flux is higher with TRIPOLI-4® than with DARWIN3-SFR. In this energy range, the  $^{240}\text{Pu}$  has a high capture cross section, which leads to different reaction rates estimations between the two codes and impacts the calculated production of  $^{241}\text{Pu}$  and  $^{242}\text{Pu}$ .

Table 3: Average DOUBLON plutonium isotopic ratios

$^{239}\text{Pu}/^{238}\text{U}$	$^{240}\text{Pu}/^{239}\text{Pu}$	$^{241}\text{Pu}/^{239}\text{Pu}$	$^{242}\text{Pu}/^{239}\text{Pu}$
$\sim 3.5 E^{-2}$	$\sim 4.5 E^{-2}$	$\sim 1.0 E^{-3}$	$\sim 5.0 E^{-5}$

## 4.5 Comparative analysis of the DARWIN3-SFR and DARWIN-2 results

A comparison of the experimental values to those obtained with DARWIN3-SFR and DARWIN-2 is performed. In both cases only the concentrations of the DOUBLON pins are depleted, the core temperature is 650 ° C and the JEFF-3.1.1 nuclear data library is used.

### 4.5.1 Calculations with the DARWIN-2 depletion package

A previous interpretation of DOUBLON was performed some years ago (Lebrat et al., 2015) with the DARWIN-2 depletion package, using the ERANOS neutronic code (Ruggieri et al., 2006), the PEPIN2 depletion module and the JEFF-3.1.1 nuclear data library.

The cell calculations were performed with the ECCO module (Rimpault, 1995), using a spatially heterogeneous subassembly description and a 1968 energy groups mesh. The FEG58 subassembly environment modification was taken into account during the core calculation, that was performed with the VARIANT (Carrico et al., 1992) solver of ERANOS, in a 33 groups energy mesh.

Once the reaction rates and neutron spectrum have been calculated with ERANOS for each reactor cycle and each pin, the PEPIN2 module was used to perform the depletion. This is the sequence called DARWIN-2, which permits to obtain the final concentration of each isotope inside the samples. A flux adjustment of +1% in the calculation was necessary to match the  $^{148}\text{Nd}$  production measured in the experiment.

### 4.5.2 Comparative analysis of the $^{148}\text{Nd}$ production

The C/E obtained for the  $^{148}\text{Nd}/^{238}\text{U}$  isotopic ratio are shown in Figure 18. We can observe that:

- The average C/E of the  $^{148}\text{Nd}/^{238}\text{U}$  ratio is similar between DARWIN-2 and DARWIN3-SFR: on average, the burnup level (i.e. the neutron flux level) calculated by the two codes in the whole fertile blanket is similar.
- There is, however, a very large pin-to-pin spatial variation. In addition, the shape of the  $^{148}\text{Nd}/^{238}\text{U}$  C/E is very different between DARWIN-2 and DARWIN3-SFR, especially at the interface between the two fertile subassemblies.

The pins are located at increasing distances from the center of the core (Figure 11), and the flux level decreases inside the blanket because the neutrons are captured by the  $^{238}\text{U}$ . This means that the farther the pin, the lower the neutron flux level and hence the fission rate, which tends to decrease the  $^{148}\text{Nd}$  production. But when neutrons penetrate the fertile blanket, they are also being slowed down by diffusion reactions and the decrease of their energy makes them more likely to provoke a fission of  $^{235}\text{U}$  or  $^{239}\text{Pu}$ , which tends to increase the  $^{148}\text{Nd}$  production.

This suggests that the estimation of the neutron energy evolution inside the blanket is a key point for an accurate calculation of the  $^{148}\text{Nd}/^{238}\text{U}$  ratio and thus of the other isotopic ratios.

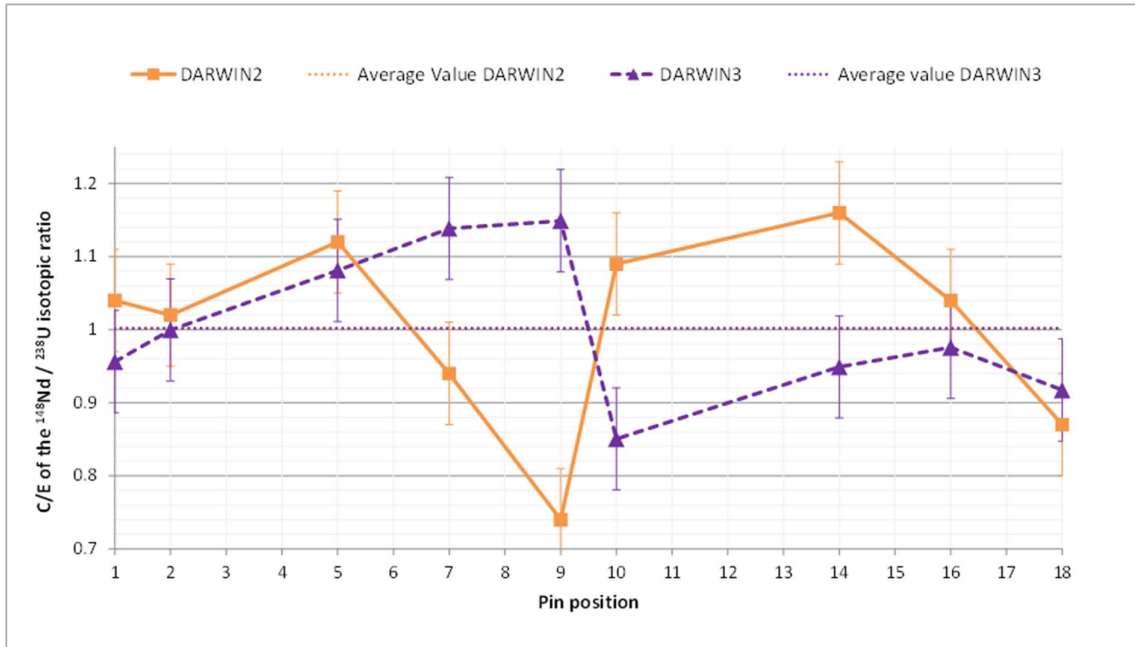


Figure 18: C/E of the  $^{148}\text{Nd}/^{238}\text{U}$  isotopic ratio obtained with DARWIN-2 and DARWIN3-SFR

#### 4.5.3 Analysis of the effect of the neutron energy spectrum calculation

To analyze the neutron energy spectrum in a 33 groups energy mesh, we calculate the normalized neutron flux  $\phi_{norm}^g$ , which is the neutron flux  $\phi^g$  of the energy group  $g$  divided by the sum over all the groups  $\sum \phi^g$ .

Figure 19 and 20 present the (spatial) average neutron energy spectrum calculated with DARWIN-2 and DARWIN3-SFR inside the fertile blanket. We notice that the spectra obtained with both codes are globally similar, although a bit softer with DARWIN3-SFR.

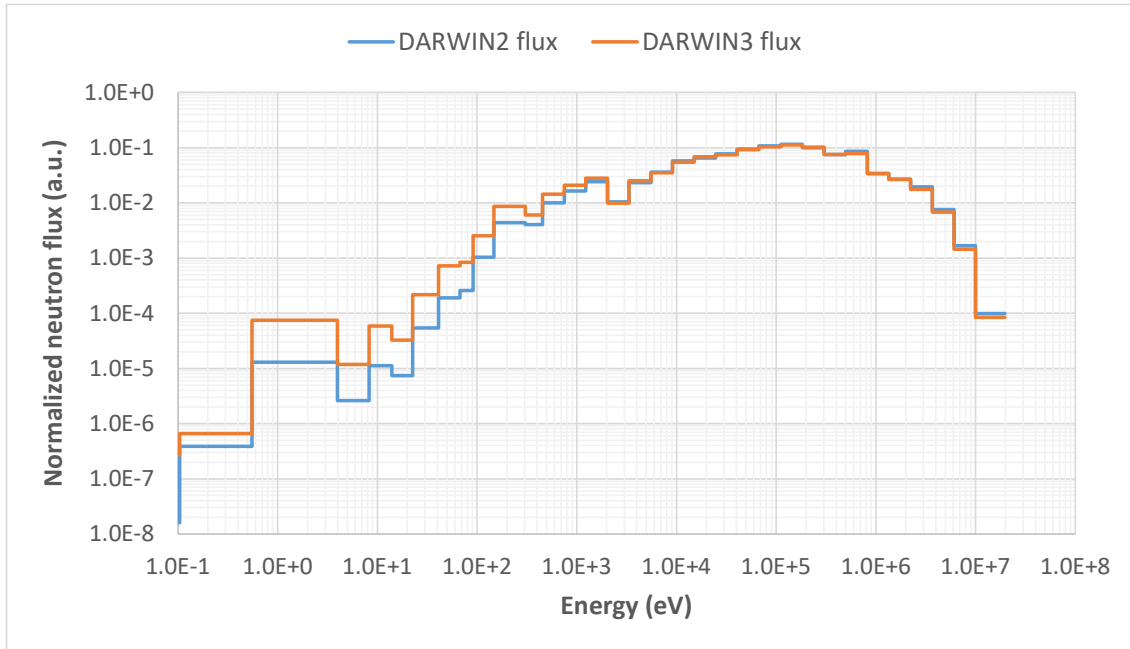


Figure 19: DARWIN-2 and DARWIN3-SFR spatial average normalized neutron flux (logarithmic scale)

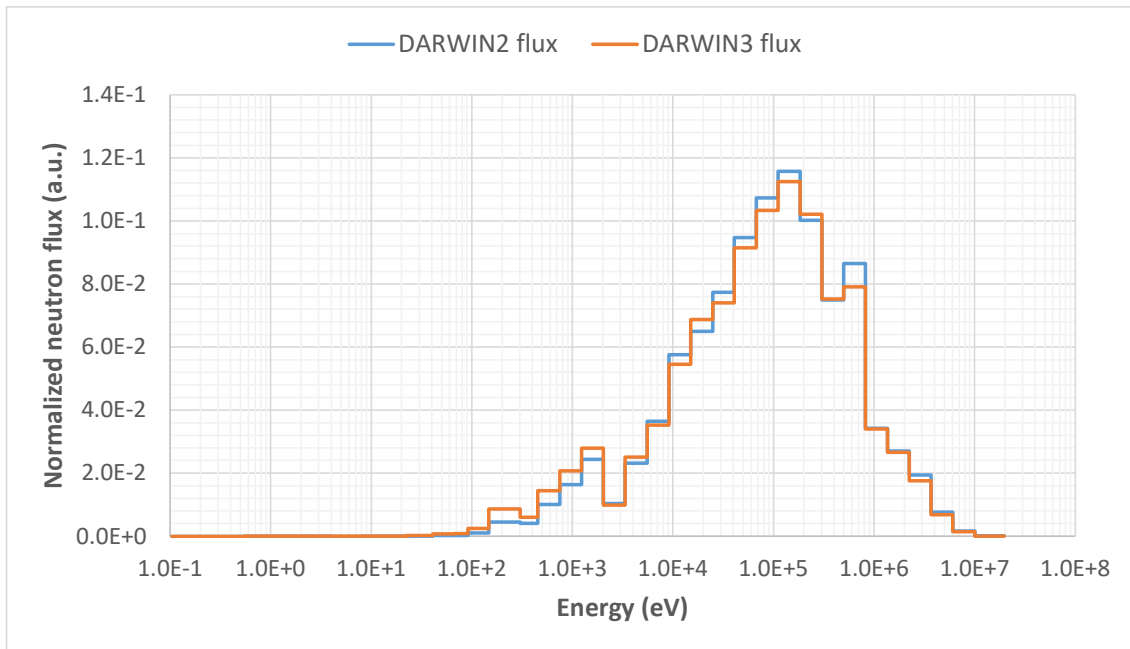


Figure 20: DARWIN2 and DARWIN3-SFR spatial average normalized neutron flux (linear scale)

#### 4.5.4 Analysis of the $^{238}\text{U}$ reactions cross sections

The differences observed in the calculated neutron energy spectrum indicates that we need to study the cross sections of some  $^{238}\text{U}$  reactions, especially the capture and fission. Figure 21 compares the values of those cross sections in DARWIN3-SFR and DARWIN-2: the cross-section values were recovered in the calculation codes ERANOS and APOLLO3® for a 33-group energy mesh and the curve represents the APOLLO3® / ERANOS ratio.

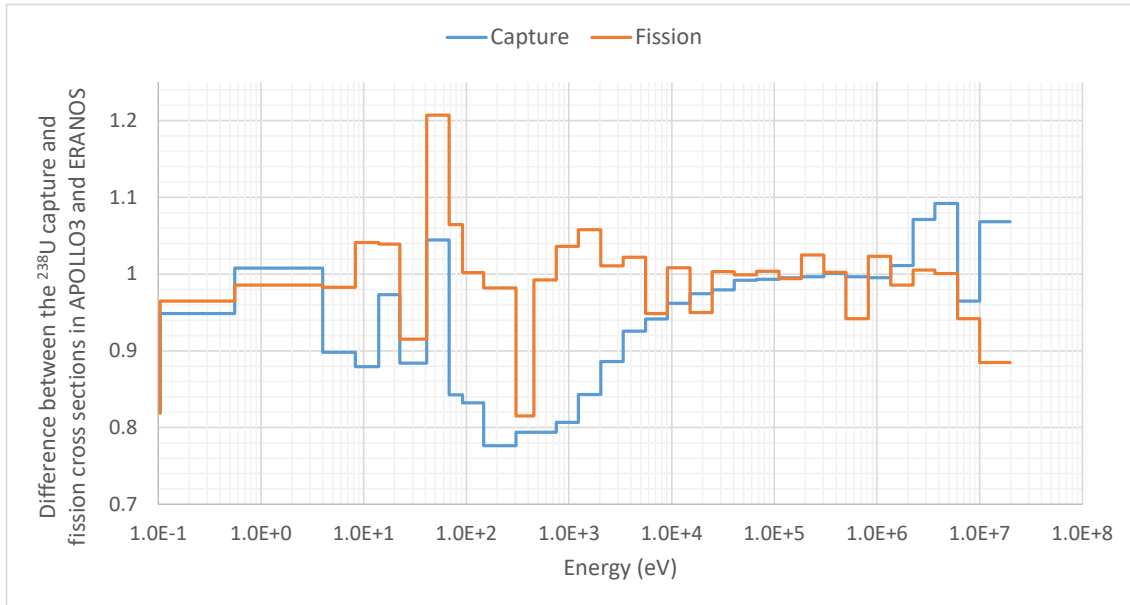


Figure 21: Difference between the  $^{238}\text{U}$  capture and fission cross sections in APOLLO3® and ERANOS

There are significant differences between DARWIN3-SFR and DARWIN-2, over the entire energy range, both for the capture and the fission cross section of  $^{238}\text{U}$ . These differences may explain the disparities in the calculated  $^{148}\text{Nd}/^{238}\text{U}$  ratio, as the  $^{148}\text{Nd}$  is produced by the (energy dependent) fission of the  $^{239}\text{Pu}$  generated by the (energy dependent) capture on  $^{238}\text{U}$  and by the (energy dependent) fission of the  $^{235}\text{U}$  and  $^{238}\text{U}$ .

For subcritical mediums such as the fertile blanket, ERANOS uses a calculation scheme based on many approximations, which can induce biases for obtaining of the 33 energy group cross sections used for the core calculation. On the other hand, a lot of work has been carried out with APOLLO3® in order to improve the calculation schemes for subcritical mediums (Garcia et al., 2019). It seems that the generation of the cross sections for the subcritical mediums is a key point, which needs more calculation and experimental validation.

#### 4.5.5 Other isotopic ratios

Despite significant pin-to-pin disparities, the average C/E of the  $^{148}\text{Nd}/^{238}\text{U}$  is close to one over the whole radial fertile blanket, allowing us to interpret the other isotopic ratios by averaging the values obtained over the pins. Figure 22 shows the C/E of the average isotopic ratios obtained with DARWIN-2 and DARWIN3-SFR; the associated uncertainties mainly result from the pin-to-pin dispersion.

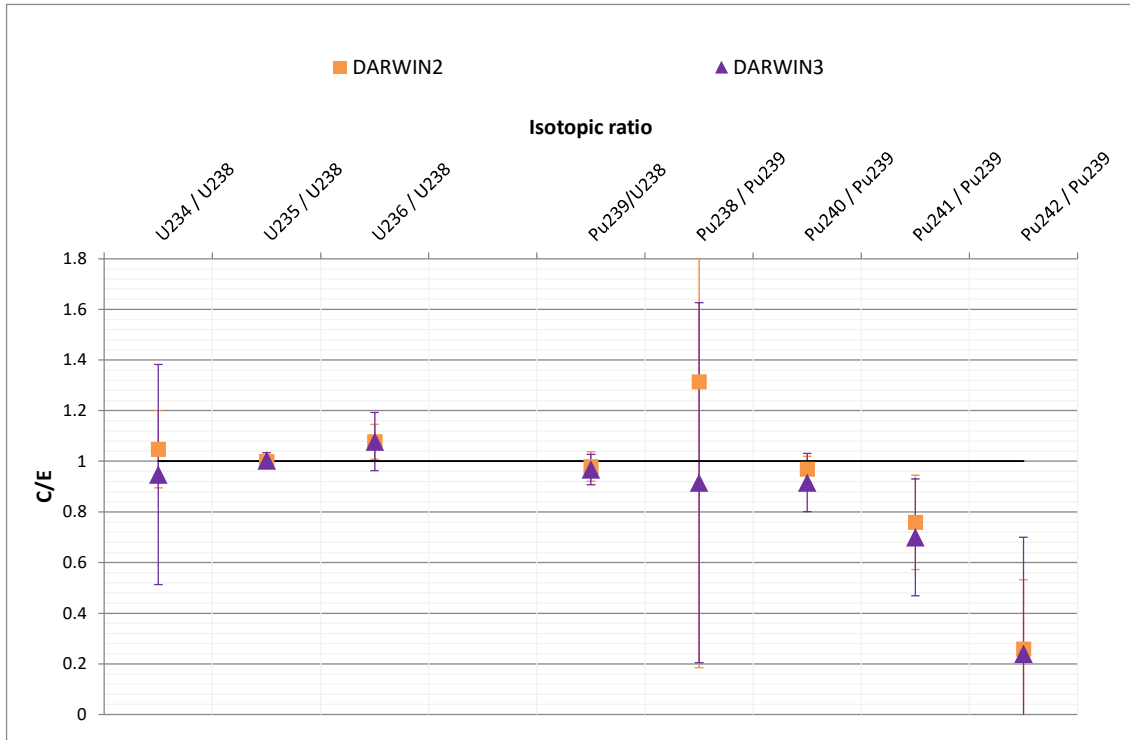


Figure 22: C/E of the average isotopic ratios estimated with DARWIN-2 and DARWIN3-SFR

We observe on Figure 22 that:

- The average  $^{234}\text{U}$ ,  $^{235}\text{U}$  and  $^{236}\text{U}$  productions show a good agreement between the two depletion codes and the experiment.
- The average production of  $^{239}\text{Pu}$  is also very well estimated, which is consistent with the fact that the average C/E of  $^{148}\text{Nd}/^{238}\text{U}$  is close to one.
- The average production of  $^{240}\text{Pu}$  - which results from the capture on  $^{239}\text{Pu}$  - is also correctly calculated.
- The  $^{238}\text{Pu}$  production shows better results with DARWIN3-SFR than with DARWIN-2, but the uncertainties are important because of the large pin-to-pin dispersion of the  $^{238}\text{Pu}/^{239}\text{Pu}$  ratio.
- The productions of  $^{241}\text{Pu}$  and  $^{242}\text{Pu}$  are consistent between DARWIN-2 and DARWIN3-SFR. However, they are not compatible with the measurements, which confirms the complexity for the depletion codes to estimate the production of these nuclides inside the fertile blanket.

#### 4.6 Impact of the nuclear data library on the calculation results

In order to evaluate the impact of the nuclear data library, we compare two DARWIN3-SFR calculations performed with JEFF-3.1.1 and JEFF-3.2 (NEA, 2016).

Figure 23 presents the C/E of the  $^{148}\text{Nd}/^{238}\text{U}$  ratio in both cases. We can observe that there is a slight difference for the first pins of the fertile blanket - inside the FEF79 subassembly - but that the results are similar for the FEG58 subassembly. The limited increase of the C/E value in the FEF79 assembly with JEFF-3.2 implies an average value of the C/E that is very slightly higher and closer to one.



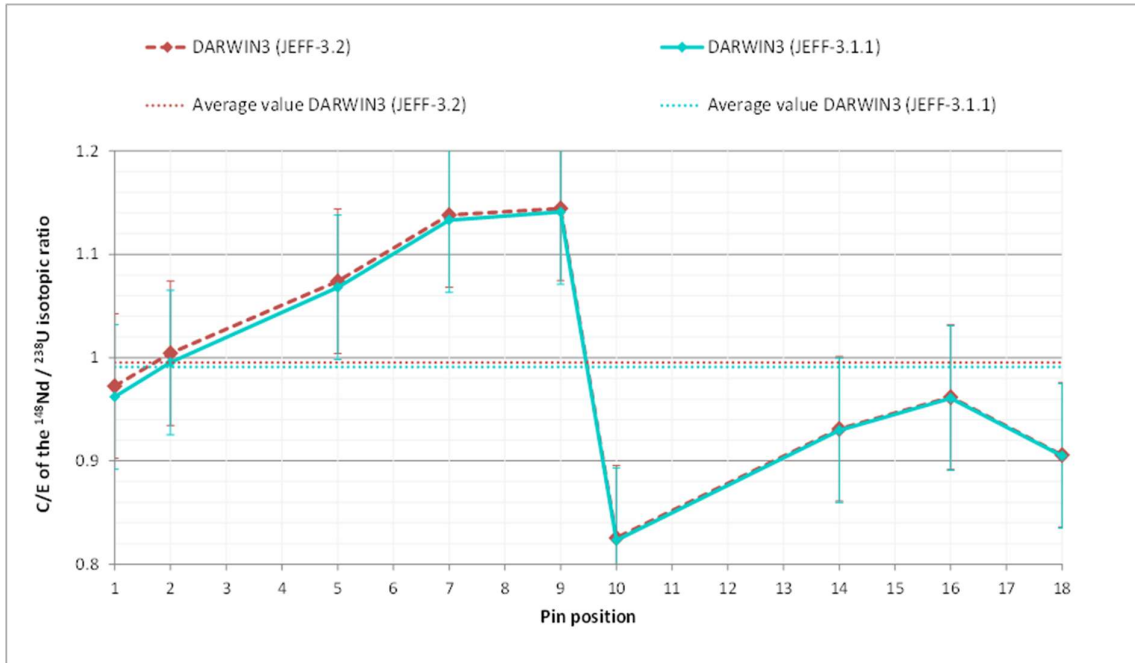


Figure 23: C/E of the  $^{148}\text{Nd}/^{238}\text{U}$  isotopic ratio calculated with DARWIN3-SFR using the JEFF-3.1.1 or the JEFF-3.2 nuclear data library

Figure 24 presents the C/E values for the other isotopic ratios. We can observe that the results are similar for the uranium isotopes and the  $^{239}\text{Pu}$ . Some differences are observed for the  $^{238}\text{Pu}$ ,  $^{241}\text{Pu}$  and  $^{242}\text{Pu}$ , but the results are compatible with each other given their uncertainties.

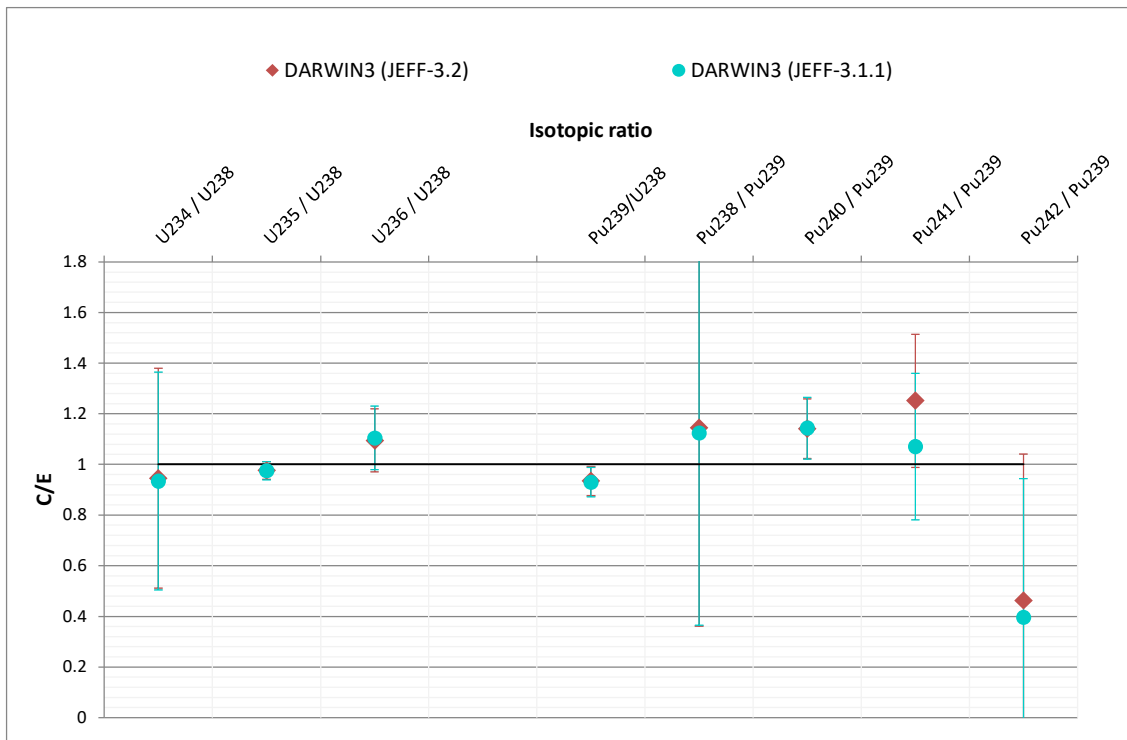


Figure 24: C/E of the DOUBLON isotopic ratios estimated with DARWIN3-SFR using the JEFF-3.1.1 or the JEFF-3.2 nuclear data library

We notice in Figure 25 that there are significant variations in the capture cross sections of  $^{240}\text{Pu}$  when changing the nuclear data library. Indeed, this cross section has a much larger resonance with JEFF-3.2 than with JEFF-3.1.1. We also notice that the neutron spectrum calculated with DARWIN3-SFR is softer with JEFF-3.1.1 than with JEFF-3.2, which explains that the production of  $^{241}\text{Pu}$  and  $^{242}\text{Pu}$  differ.

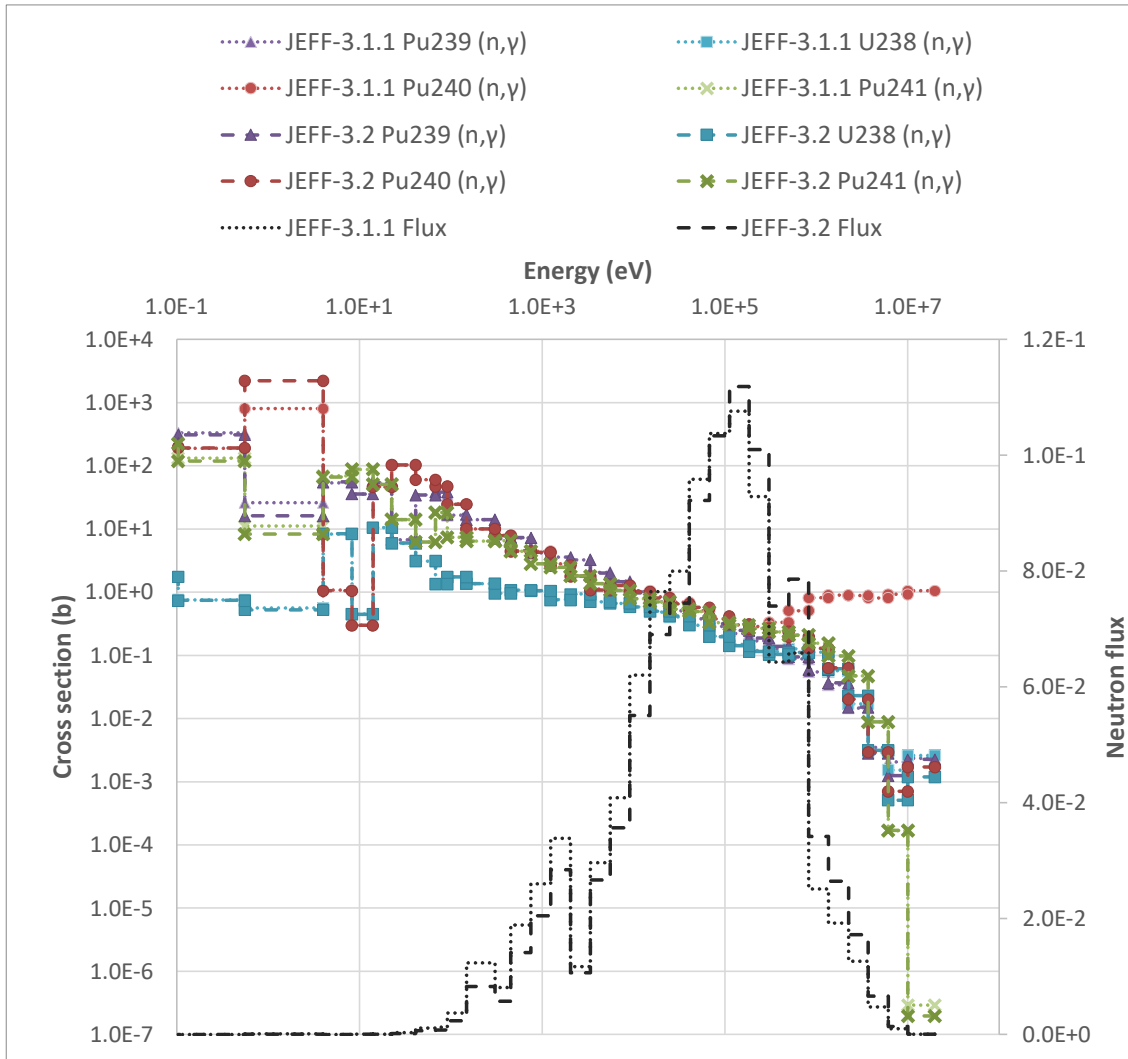


Figure 25: Comparison of the neutron flux and some capture reactions cross sections calculated with DARWIN3-SFR using JEFF-3.1.1 and JEFF-3.2

#### 4.7 Impact of the temperature on the calculation results

Two DARWIN3-SFR calculations - performed with a temperature of 20°C and 650°C - are compared in order to estimate the impact of temperature.

The corresponding C/E values of the  $^{148}\text{Nd}/^{238}\text{U}$  isotopic ratio are shown in Figure 26. We can observe that the results are identical for the first subassembly FEF79 (pins 1 to 9), but that the temperature affects the results in the second subassembly FEG58 (pins 10 to 18).

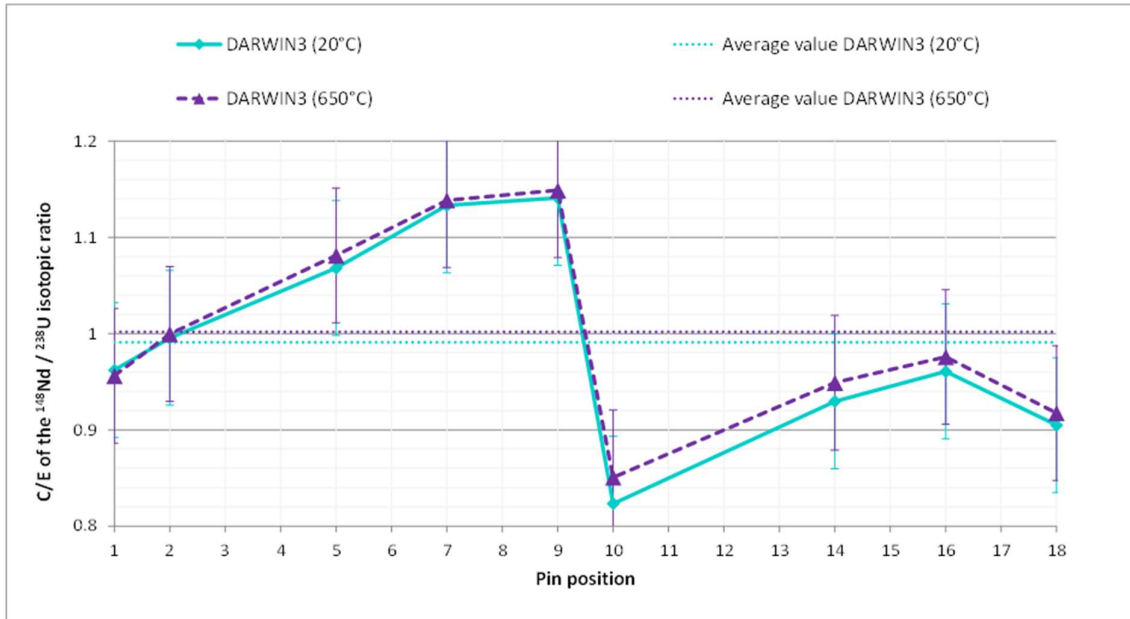


Figure 26: C/E of the  $^{148}\text{Nd}/^{238}\text{U}$  isotopic ratio calculated with DARWIN3-SFR and a temperature of 20°C or 650°C

The C/E results for the other isotopic ratios are shown in Figure 27. We can observe that the results are similar for  $^{234}\text{U}$ ,  $^{235}\text{U}$ ,  $^{236}\text{U}$  and  $^{239}\text{Pu}$ , but that there are some differences for  $^{238}\text{Pu}$ ,  $^{240}\text{Pu}$ ,  $^{241}\text{Pu}$  and  $^{242}\text{Pu}$ .

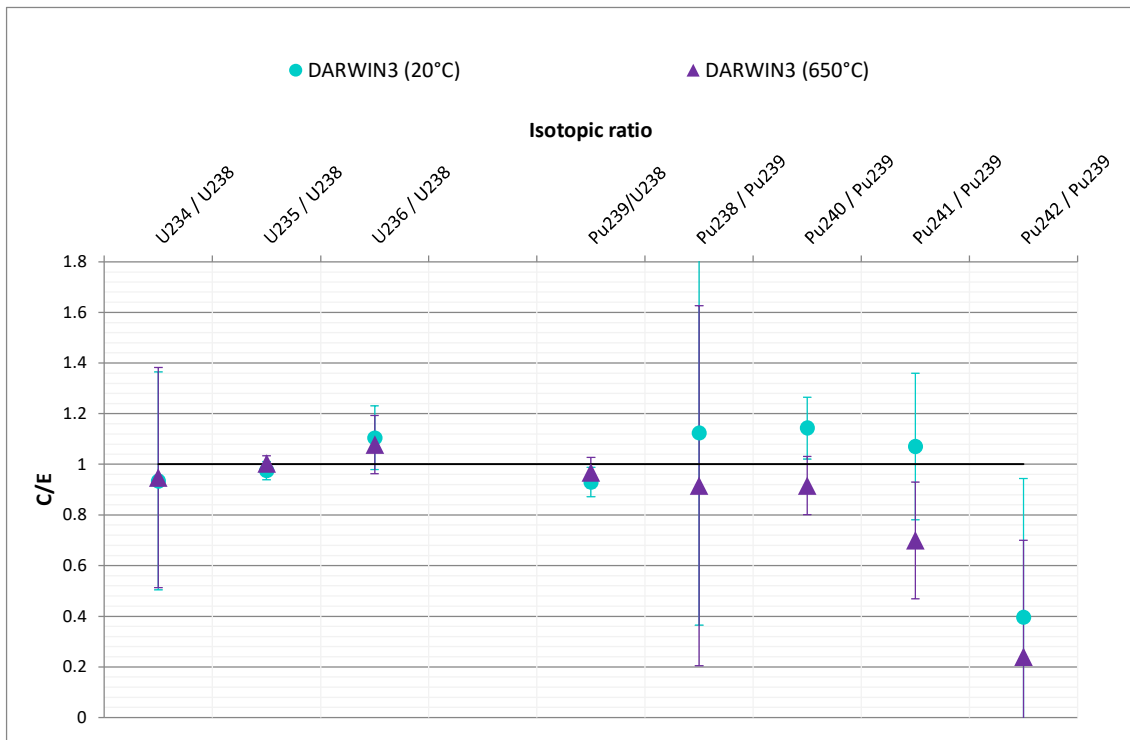


Figure 27: C/E of the isotopic ratios calculated with DARWIN3-SFR and a temperature of 20°C or 650°C

Figure 28 and 29 show the impact of the temperature on some capture reactions cross sections and on the DARWIN3-SFR calculated neutron flux. We notice that there is a slight effect of temperature on the neutron flux and a significant effect on the  $^{240}\text{Pu}$  capture cross section, which impacts the production of  $^{241}\text{Pu}$  and  $^{242}\text{Pu}$ .

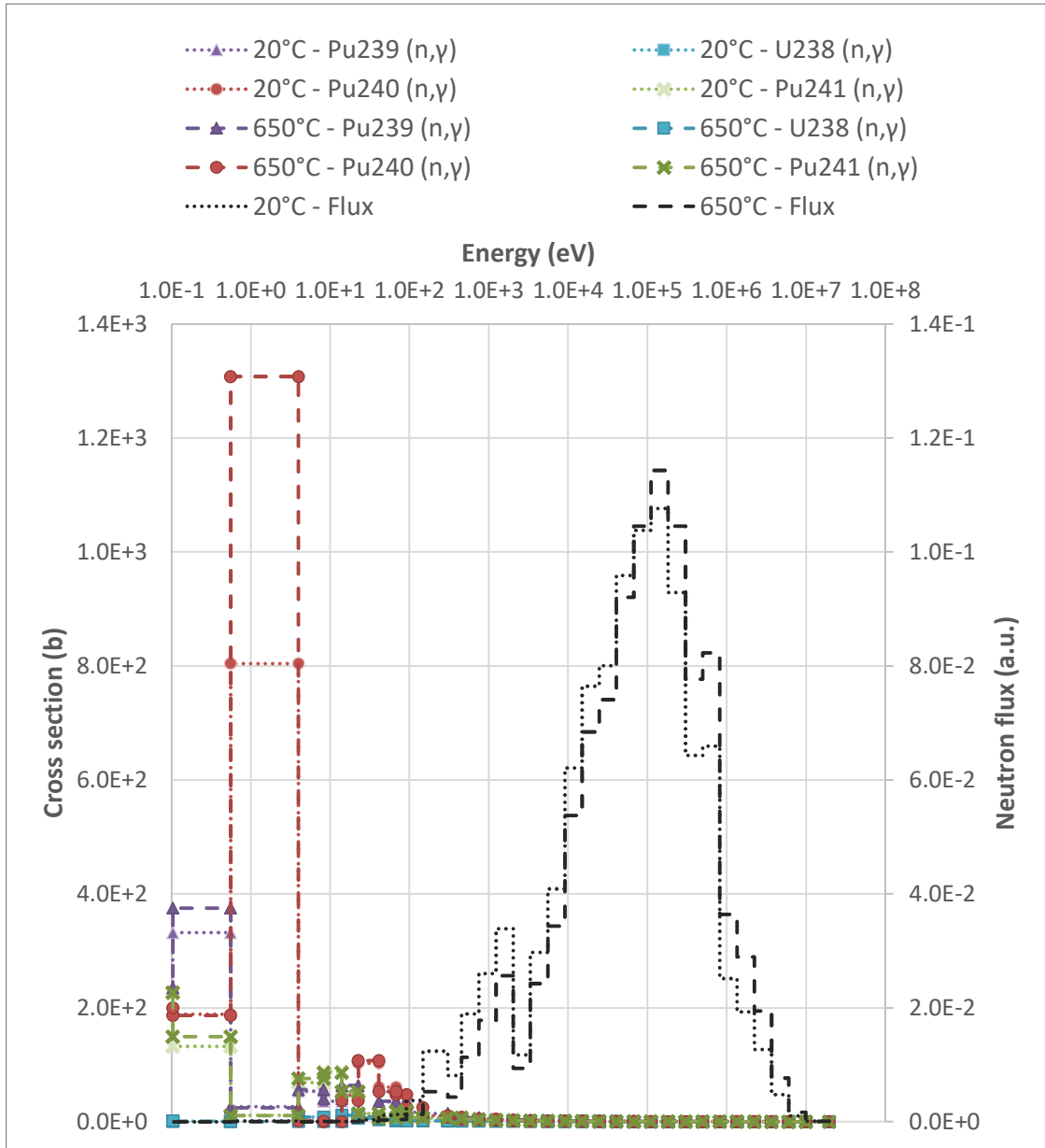


Figure 28: Comparison of the neutron flux and some capture reactions cross sections calculated with DARWIN3-SFR and a temperature of 20°C and 650°C (linear scale)

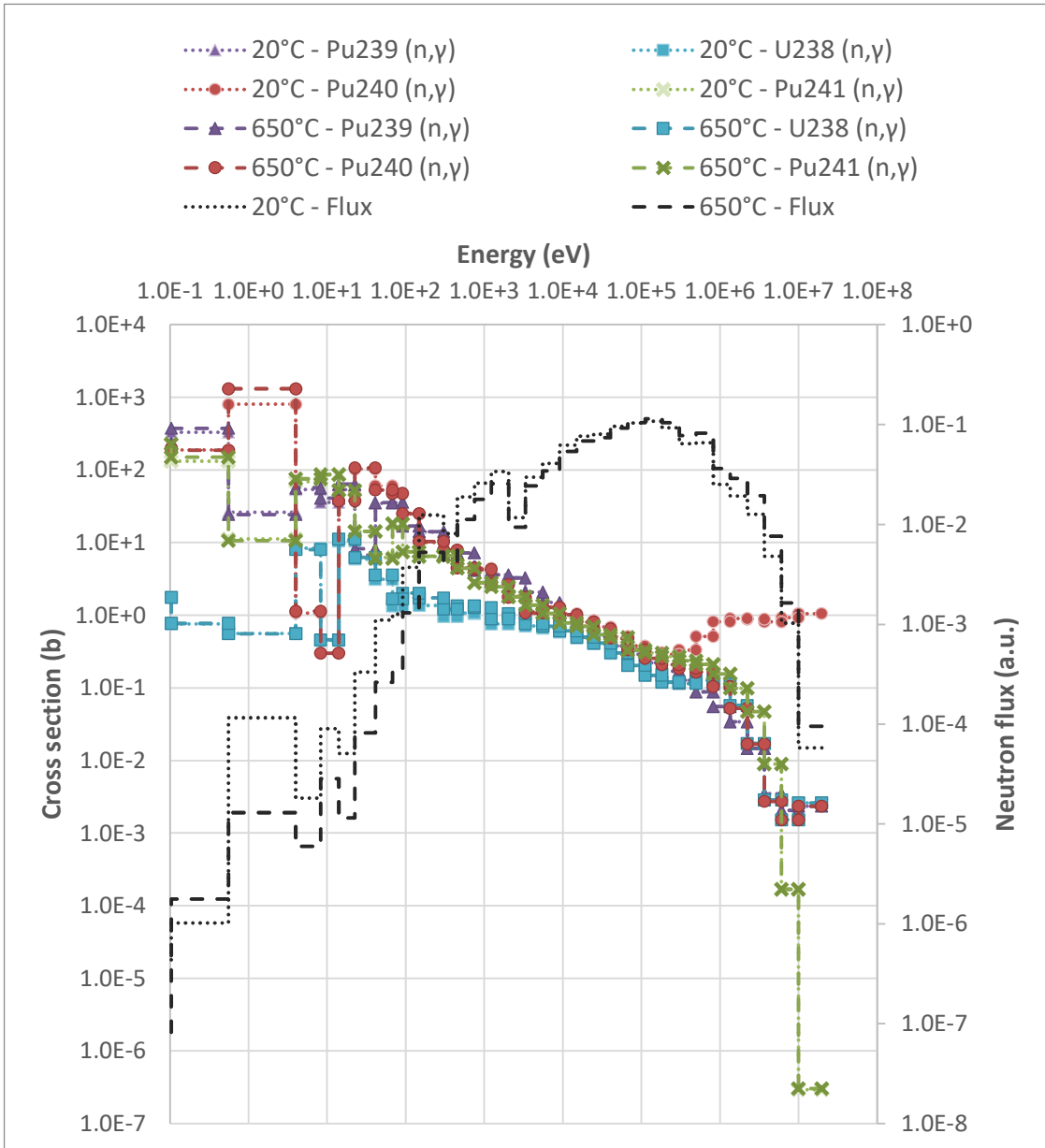


Figure 29: Comparison of the neutron flux and some capture reactions cross sections calculated with DARWIN3-SFR and a temperature of 20°C and 650°C (logarithmic scale)

## 5. Conclusion

DARWIN3-SFR is the CEA fuel depletion package that aims to be the new reference for deterministic calculations. It is composed of the deterministic neutronic code APOLLO3® and the depletion module MENDEL and needs to be validated by comparison with experimental results and other calculation tools. The DARWIN3-SFR package benefits from a reasonable calculation time and the independent use of the two codes (APOLLO3® and MENDEL) makes it possible to manage easily the generation of the MPOs output files and to perform user-friendly neutron flux adjustments.

We have used DARWIN3-SFR to revisit the DOUBLON experiment and we have compared our calculations to the measurements, to the previous results obtained with DARWIN-2 and to reference calculations performed with the stochastic code TRIPOLI-4®. This experiment consisted in the irradiation of two subassemblies located in the first and second row of the radial fertile blanket of the sodium-cooled fast reactor PHENIX. They were irradiated during a few cycles from 1979 to 1981. Nine pins were analyzed and provided some isotopic ratios, useful for the validation of the depletion calculations inside the radial fertile blanket.

We observe that DARWIN3-SFR calculates the shape of the neutron flux similarly to TRIPOLI-4® within the fertile blanket, as long as a flux level adjustment is performed. However, both codes have difficulties to reproduce the fission rates. While DARWIN3-SFR and TRIPOLI-4® produce identical results for the production of most of the isotopes analyzed ( $^{234}\text{U}$ ,  $^{235}\text{U}$ ,  $^{236}\text{U}$ ,  $^{238}\text{Pu}$ ,  $^{239}\text{Pu}$  and  $^{240}\text{Pu}$ ), the difference in the neutron energy spectrum causes some disparities for the production of  $^{241}\text{Pu}$  and  $^{242}\text{Pu}$ . Indeed, the low-energy flux is higher with TRIPOLI-4® than with DARWIN3-SFR in the energy range where the  $^{240}\text{Pu}$  has a high capture cross section. Nevertheless, it must be emphasized that these nuclides are produced in a very small amount during the irradiation.

DARWIN3-SFR and DARWIN-2 are, on average, efficient at calculating the neutron flux level over the entire fertile blanket. However, the two codes show a strong pin-to-pin dispersion, resulting in a different shape of the neutron flux inside the blanket. With DARWIN3-SFR, the neutron spectrum is softer than in DARWIN-2 and there are also discrepancies in the  $^{238}\text{U}$  capture and fission cross sections in both codes.

The temperature has an impact on the calculation of the production of all the plutonium isotopes: it has a slight impact on the flux level, but more noticeably on the  $^{240}\text{Pu}$  capture cross section.

Concerning the choice of the nuclear data library, it has an impact on the calculation of the production of  $^{241}\text{Pu}$  and  $^{242}\text{Pu}$ , because it strongly influences the  $^{240}\text{Pu}$  capture cross section.

## References

- Archier, P. et al., 2014. COMAC: Nuclear Data Covariances Matrices Library for Reactor Application. Proceedings of PHYSOR 2014, Kyoto, Japan.
- Baudron, A.-M. and Lautard, J.-J., 2007. MINOS: a Simplified Pn Solver for Core Calculations. Nuclear Science and Engineering, vol. 155, pp. 250-263.  
<https://doi.org/10.13182/NSE07-A2660>
- Beltranda, G., 1974. Etude des couvertures et réflecteurs des réacteurs de la filière à neutrons rapides. Thèse du 3ème cycle, Grenoble.
- Brun, E. et al., 2015. TRIPOLI4®, CEA, EDF and AREVA reference Monte-Carlo code. Annals of Nuclear Energy, 82, 151-160.
- Calame, A., Lebrat, J.-F., Buiron, L., 2021. Analysis of the TRAPU irradiation in PHENIX with TRIPOLI-4® and DARWIN3-SFR for the Validation of Fast Reactor fuel depletion Calculations. Annals of Nuclear Energy, Volume 157, 108167.  
<https://doi.org/10.1016/j.anucene.2021.108167>
- Carrico, B. et al., 1992. Three-Dimensional Variational Nodal Transport Methods for Cartesian, Triangular, and Hexagonal Criticality Calculations. Journal of Nuclear Science and Engineering, Volume 111.
- Corcuera, R., 1974. Méthodes Théoriques pour le Calcul Neutronique des Systèmes Cœur-Couverture et Cœur-Réflecteur des Réacteurs à Neutrons Rapides. Thèse de l'Université de Paris-Sud.
- Eschbach, R. et al., 2008. Improvement of the Experimental Validation of the DARWIN code system due to the JEFF-3.1 Library for UOX Spent Fuel Inventory and Decay Heat Calculation. Proceedings of PHYSOR'08, Interlaken, Switzerland.
- Grimm, K.N. et al., 1998. Comparison of measured and calculated composition of irradiated EBR-II blanket assemblies. International Conference on the Physics of Nuclear Science and Technology, Islandia, Long Island, New York.
- Hill, R.N., 1997. An Analysis of Deficiencies in Fast Reactor Blanket Physics Predictions. Ph.D. Thesis, Purdue University.
- NEA, 2016. The JEFF-3.2 Nuclear Data Library  
[https://www.oecd-nea.org/dbforms/data/eva/evatapes/jeff\\_32/](https://www.oecd-nea.org/dbforms/data/eva/evatapes/jeff_32/)
- Garcia, E. et al., 2019. Flux distribution of the Superphenix start-up core for the validation of neutronic codes. Annals of Nuclear Energy 133:889-899.  
<https://doi.org/10.1016/j.anucene.2019.06.066>
- Lahaye, S. et al., 2014. First verification and validation steps of MENDEL release 1.0 cycle code system. Proceeding of PHYSOR 2014, Kyoto, Japan.

Lahaye, S. et al., 2018. Uncertainty quantification of isotopic densities in depleted fuel. Proceedings of ANS Best Estimate Plus Uncertainty International Conference (BEPU 2018), Real Collegio, Lucca, Italy.

Lebrat, J.-F. et al., 2011. JEFF-3.1.1 Nuclear Data Validation for Sodium Fast Reactors“, Journal of Nuclear Science and Technology, 48, No 4.  
<https://www.tandfonline.com/doi/pdf/10.1080/18811248.2011.9711742>

Lebrat, J.-F. et al., 2015. Analysis of the TRAPU and DOUBLON irradiations in PHENIX for the experimental validation of the DARWIN package for fast reactors. Proceedings of Global 2015, Paris (France).  
<https://hal-cea.archives-ouvertes.fr/cea-02509740/document>

Lebrat, J.-F. et al., 2018. Uncertainty assessment on the calculated decay heat of the ASTRID basic design core based on the DARWIN-2.3 package. Annals of Nuclear Energy 120, 378-391.  
<https://doi.org/10.1016/j.anucene.2018.05.043>

Lewis, E.-E. and Dilber, I., 1986. Finite Element, Nodal and Response Matrix Methods: a Variational Synthesis for Neutron Transport. Progress in Nuclear Energy, vol. 18, n° 11/2, pp. 63-74.

Moller, J.-Y. et al., 2011. Minaret, a deterministic neutron transport solver for nuclear core calculations. Proceedings of M&C, Rio de Janeiro, Brazil.

Rimpault, G., 1995. Algorithmic features of the ECCO cell code for treating heterogeneous fast reactor assemblies. Proc. Int. Conf. on Mathematics and Computation, M&C95, Portland, Oregon, USA.

Ruggieri, J.M., Tommasi, J., Lebrat, J.-F., Suteau, C., Plisson-Rieunier, D., De Saint-Jean, C., Rimpault, G., Sublet, J.C., 2006. ERANOS 2.1: International Code System for GEN IV Fast Reactor Analysis. Proceedings of ICAPP '06, Reno, NV, USA.

San-Felice, L. et al., 2013. Experimental Validation of the DARWIN2.3 package for Fuel Cycle Applications. Nuclear Technology, 184.

Santamarina, A. et al, 2009. The JEFF-3.1.1 Nuclear Data Library. JEFF Report 22, NEA 6807, Organization for Economic Cooperation and Development.

Schneider, D. et al., 2016. APOLLO3®: CEA/DEN multi-purpose code for reactor physics analysis. Proceedings of PHYSOR 2016, Sun Valley, ID, USA.

Soule, R., 1982. Définition et validation d'un formulaire neutronique pour l'étude des propriétés des couvertures des réacteurs à neutrons rapides. Thèse de l'Université d'Orsay.

Tsilanizara, A. et al., 2000. DARWIN: an evolution code system for a large range applications. Journal of Nuclear Science and Technology, Supplement 1, 845-849.

Vaglio-Gaudard, C., Bellier, P., Buiron, L., Lahaye, S., Lebrat, J.-F., Miranda, P., Roque, B., Tsilanizara, A., 2016. Development of the DARWIN3-SFR Fuel Cycle Tool for Decay Heat Calculations in New Fast Reactors. Proceedings PHYSOR 2016, Sun Valley, Idaho, USA.

Vidal, J.-F. et al., 2017. APOLLO3 homogenization techniques for transport core calculations, application to the ASTRID CFV core. Nucl. Eng. Technol., vol.49, pp.1379-1387.